Article type : MS - Regular Manuscript

Author Manuscript

New insights into the covariation of stomatal, mesophyll and hydraulic conductances from optimisation models incorporating non-stomatal limitations to photosynthesis

Roderick Dewar[1], Aleksanteri Mauranen[2], Annikki Mäkelä[3], Teemu Hölttä[3], Belinda Medlyn[4] and Timo Vesala[2,3]

[1]Plant Sciences Division, Research School of Biology, The Australian National University, Canberra ACT 2601, Australia; [2]Department of Physics, PO Box 68, FI-00014, University of Helsinki, Finland; [3]Department of Forest Sciences, PO Box 27, FI-00014, University of Helsinki, Finland; [4]Hawkesbury Institute for the Environment, Western Sydney University, Locked Bag 1797, Penrith NSW 2751, Australia

Author for correspondence:
Roderick Dewar
Tel: +61 2 61252447
Email: roderick.dewar@anu.edu.au

Received: *13 June 2017*
Accepted: *10 September 2017*

Summary

- Optimisation models of stomatal conductance (g_s) attempt to explain observed stomatal behaviour in terms of cost-benefit trade-offs. While the benefit of stomatal opening through increased CO_2 uptake is clear, currently the nature of the associated cost(s)

This is the author manuscript accepted for publication and has undergone full peer review but has not been through the copyediting, typesetting, pagination and proofreading process, which may lead to differences between this version and the Version of Record. Please cite this article as doi: 10.1111/nph.14848

This article is protected by copyright. All rights reserved

remains unclear. We explored the hypothesis that g_s maximises leaf photosynthesis, where the cost of stomatal opening arises from non-stomatal reductions in photosynthesis induced by leaf water stress.

- We analytically solved two cases, CAP and MES, in which reduced leaf water potential leads to reductions in, respectively, carboxylation CAPacity and MESophyll conductance (g_m).
- Both CAP and MES predict the same one-parameter relationship between the intercellular-to-atmospheric CO_2 concentration ratio (c_i /c_a) and vapour pressure deficit (D), viz. c_i /$c_a \approx \xi/(\xi + \sqrt{D})$, as that obtained from previous optimisation models, with the novel feature that the parameter ξ is determined unambiguously as a function of a small number of photosynthetic and hydraulic variables. These include soil-to-leaf hydraulic conductance, implying a stomatal closure response to drought. MES also predicts that g_s/g_m is closely related to c_i /c_a and is similarly conservative.
- These results are consistent with observations, give rise to new testable predictions, and offer new insights into the covariation of stomatal, mesophyll and hydraulic conductances.

Key words: hydraulic conductance, mesophyll conductance, model, non-stomatal limitation, optimisation, photosynthesis, stomatal conductance, trait covariation.

Introduction

Leaf stomata play a central role in mediating the exchange of CO_2 and water vapour between the atmosphere and the global land surface. Therefore, understanding the responses of stomatal conductance (g_s) to changes in atmospheric CO_2 concentration, air/soil water deficits and other environmental variables is crucial to predicting global change impacts on the coupled climate-vegetation system. The challenge for modellers is that stomatal behaviour cannot be understood in isolation, because g_s is tightly coupled to other plant and soil variables such as mesophyll conductance (Flexas *et al.*, 2008) and soil-to-leaf hydraulic conductance (Sperry *et al.*, 1993; Rodriguez-Dominguez *et al.*, 2016), which covary with g_s on a range of timescales. Ultimately a whole-system perspective is called for. Optimisation models provide an integrative approach to understanding whole-plant responses to global change, in which adaptation for maximum fitness acts as a guiding organisational principle (e.g. Dewar *et al.*, 2009; Franklin *et al.*, 2012).

This article is protected by copyright. All rights reserved

Author Manuscript

Optimisation models of stomatal conductance have shown some success in synthesising stomatal responses to environmental change (e.g. Cowan, 1977, 1982, 1986; Cowan & Farquhar, 1977; Givnish, 1986; Hari *et al.*, 1986; Friend, 1991, 1995; Mäkelä *et al.*, 1996; Katul *et al.*, 2010; Medlyn *et al.*, 2011, 2013; Manzoni *et al.*, 2013; Prentice *et al.*, 2014; Sperry *et al.*, 2016; Wang *et al.*, 2016; Wolf *et al.*, 2016; Hölttä *et al.*, 2017), although challenges remain with regard to modelling responses to CO_2 (Medlyn *et al.*, 2013) and drought (Zhou *et al.*, 2013). Conceptually, optimisation models of g_s are attractive because, unlike empirical models (e.g. Jarvis, 1976; Ball *et al.*, 1987; Collatz *et al.*, 1991; Leuning, 1995), they offer an explanation of stomatal behaviour in terms of the trade-off between the costs and benefits of stomatal opening, while avoiding the complexities and uncertainties of more mechanistic models whose parameter values are not easily determined experimentally (e.g. Dewar, 1995, 2002; Buckley *et al.*, 2003).

Current uncertainties in stomatal optimisation models

Nevertheless, while the benefit of stomatal opening through increased CO_2 uptake is clear, currently the specific nature of the associated cost(s) remains unclear. This uncertainty limits not only the theoretical understanding that optimisation models of g_s currently provide, but also their practical implementation within larger-scale models, such as dynamic vegetation models for predicting climate change impacts on the biosphere (e.g. Sitch *et al.*, 2008; Fisher *et al.*, 2010). Two examples of current stomatal optimisation models serve to illustrate these uncertainties.

First, according to a long-standing hypothesis (Cowan & Farquhar, 1977), the optimal diurnal variation of stomatal conductance is one that maximises the time integral of $A - E/\lambda$, where A and E are photosynthesis and transpiration, respectively, and λ (mathematically, a Lagrange multiplier) is equal to the marginal water loss of plant carbon gain ($\partial E/\partial A$) at the optimal operating point. Uncertainty surrounds the determination of λ and its variation over time. On short timescales λ is often treated as an undetermined constant, while on longer timescales λ has been determined from various dynamic optimisation arguments as a function of soil moisture (e.g. Cowan, 1986; Mäkelä *et al.*, 1996; Mazoni *et al.*, 2013). More recent hypotheses, in which the costs of stomatal opening have been linked in various ways to hydraulic damage (Sperry *et al.*, 2016; Wolf *et al.*, 2016), may nevertheless be viewed mathematically as versions of the Cowan–Farquhar (CF) hypothesis in which λ is a function of

This article is protected by copyright. All rights reserved

Author Manuscript

xylem water potential (and other plant variables).

In addition to these uncertainties in the determination of λ, another issue is that the CF hypothesis with constant λ predicts an unrealistic stomatal opening response to increased atmospheric CO_2 concentration (c_a) at low c_a (Hari *et al.*, 1986; Lloyd & Farquhar, 1994; Katul *et al.*, 2010). Solutions to this problem have been proposed, involving heuristic assumptions of a dependence of λ on c_a (Katul *et al.*, 2010) or *A* (Sperry *et al.*, 2016), but the justification for these assumptions remains unclear (Medlyn *et al.*, 2013). Dynamic optimisation of g_s under soil drying predicts that λ varies with c_a (Manzoni *et al.*, 2013), but the predicted dependence of λ on c_a does not lead to a realistic decline in g_s with increasing c_a (Morison & Gifford, 1983).

A second example is the Least-Cost (LC) hypothesis (Prentice *et al.*, 2014), according to which the relative cost $(a_E E + B)/A$ is minimised, where a_E is the sapwood maintenance cost per unit of transpiration, and *B* is a constant cost (i.e. independent of g_s) associated with maintenance of photosynthetic capacity. The LC hypothesis is based on the idea of an optimal carbon investment in transpiration and photosynthetic capacity which would achieve a given rate of photosynthesis at least total cost (Wright *et al.*, 2003). While this hypothesis predicts realistic diurnal stomatal responses to environmental variables (Prentice *et al.*, 2014; Wang *et al.*, 2016) including the correct closure response to increasing c_a, there is clearly a discrepancy between the timescale on which g_s varies and the timescale on which the hypothesised sapwood maintenance cost $a_E E$ varies. Therefore, the explanation of diurnal stomatal variations provided by the LC hypothesis is not clear.

Two optimisation hypotheses incorporating non-stomatal limitation to photosynthesis

What is needed, but is currently lacking, is a more transparent optimisation approach in which the costs of stomatal opening are more clearly identified and more closely related to the timescale on which stomatal conductance varies. Zhou *et al.* (2013) highlighted the need to include both stomatal and non-stomatal limitations to photosynthesis in modelling short-term responses to drought. In this paper we explore the hypothesis that the cost of stomatal opening arises from non-stomatal reductions in photosynthesis induced by lower leaf water potential (ψ_l). We examine two specific hypotheses (CAP and MES) in which stomatal opening leads (via decreased ψ_l) to reductions in carboxylation CAPacity and MESophyll conductance, respectively.

Carboxylation efficiency and capacity have been found to change appreciably in

This article is protected by copyright. All rights reserved

Author Manuscript

response to both short-term and long-term changes in vapour pressure deficit, soil water content and salinity conditions (e.g. Mooney *et al.*, 1977; O'Toole *et al.* 1977; Farquhar & von Caemmerer, 1982; Ball & Farquhar 1984a,b; Sharkey, 1984; von Caemmerer & Farquhar, 1984; Zhou *et al.* 2013, 2014). Carboxylation efficiency changes diurnally (Guo *et al.*, 2009), and midday depression of photosynthesis has been attributed to both stomatal and non-stomatal limitations to photosynthesis, even during nondrought conditions (Zhang & Gao, 2000; Mediavilla *et al.*, 2002; Nascimento & Marenco, 2013).

Mesophyll conductance (g_m) varies with environmental conditions on time scales as short as minutes (Flexas *et al.*, 2008, 2012; Kaiser *et al.*, 2015). Moreover, changes in mesophyll and stomatal conductances appear to be tightly coupled, at least on timescales associated with soil drying (Flexas & Medrano, 2002; Flexas *et al.*, 2013; Manzoni, 2014; Zhou *et al.*, 2014; Gago *et al.*, 2016). Although the mechanisms underlying variations in g_m are not well understood, contributing factors possibly include changes in carbonic anhydrase, aquaporin activity and the area of chloroplasts facing intercellular spaces (Kaiser *et al.*, 2015).

Full details of CAP and MES are given below (see Description). In view of current uncertainties about the mechanisms underlying non-stomatal limitation (NSL) to photosynthesis, for this study we viewed CAP and MES as theoretical conjectures for NSL, and explored their consequences for stomatal behaviour in the spirit of 'what-if' analysis, with the aim of stimulating further theoretical and experimental studies.

Aims

The three main aims of this study were: (1) to examine the extent to which the CAP and MES hypotheses, based on NSL to photosynthesis, can explain observed stomatal behaviour; (2) to compare predictions of CAP and MES with those of the LC and CF hypotheses, which do not involve NSL; (3) to generate new testable predictions from CAP and MES for the covariation of stomatal, mesophyll and hydraulic conductances.

Stomatal optimisation incorporating NSL to photosynthesis is not a new idea, CAP being a simplified version of earlier models (Givnish, 1986; Friend, 1991; Hölttä *et al.*, 2017). However, to our knowledge MES is new. Moreover, a novel feature of our analysis is that we solved CAP, MES, LC and CF analytically, thereby identifying the key factors that determine their behaviours. The analytical solutions also enable us to identify potential ways to experimentally distinguish between these different optimisation hypotheses, and provide simple formulae for g_s that may form a basis for improving land surface models.

This article is protected by copyright. All rights reserved

Author Manuscript

We applied each optimisation hypothesis to three photosynthesis models: a bi-substrate (light and CO_2) model (Thornley & Johnson, 1990), and the Rubisco- and light-limited branches of the photosynthesis model of Farquhar *et al.* (1980). The aim here was to make contact with previous applications of CF and LC to the Farquhar model (Medlyn *et al.*, 2011; Prentice *et al.*, 2014), and to examine how using different photosynthesis models affected the predicted stomatal behaviour.

Description

Figure 1 depicts the soil–leaf–atmosphere system considered in this study, showing the steady-state fluxes of CO_2 and H_2O and their governing equations (Eqns 1–5 below); also shown are the assumptions underlying the CAP and MES hypotheses for NSL (Eqns 6–8 below). A list of symbol definitions, units and default parameter values is given in Table 1.

Leaf C_3 photosynthesis

The rate of leaf C_3 photosynthesis (A) is assumed to be a saturating function of the chloroplast CO_2 concentration (c_c):

$$A = f\frac{c_c - \Gamma^*}{c_c + \gamma}, \qquad \text{Eqn 1}$$

where f is the CO_2-saturated rate of photosynthesis (carboxylation capacity), Γ^* is the photorespiratory compensation point, and γ is a Michaelis constant. Previous models of leaf photosynthesis (Thornley & Johnson, 1990; Farquhar *et al.*, 1980) are recovered as special cases of Eqn 1 for particular choices of f and γ (Table 2); the dependence of A on leaf irradiance (Q) may occur through f alone (e.g. the light-limited branch of the model of Farquhar *et al.*, 1980) or through both f and γ (e.g. the bi-substrate model of Thornley & Johnson, 1990). For the moment, however, we retain the generic form of Eqn 1 because the analytical predictions for stomatal conductance derived in Supporting Information Methods S1–S4 are valid for arbitrary choices of f and γ.

CO_2 and H_2O transport

For simplicity we ignore leaf mitochondrial respiration and boundary layer resistance. Then, in steady state, A (Eqn 1) is balanced by the net diffusion of CO_2 between the atmosphere and leaf

This article is protected by copyright. All rights reserved

Author Manuscript

intercellular air spaces:

$$A = g_s(c_a - c_i), \qquad \text{Eqn 2}$$

where c_a and c_i are, respectively, the atmospheric and leaf intercellular CO_2 mole fractions, and g_s is the stomatal conductance for CO_2 diffusion. We also have

$$A = g_m(c_i - c_c), \qquad \text{Eqn 3}$$

for diffusion of CO_2 between the intercellular air spaces and the chloroplasts, where c_c is the chloroplast CO_2 mole fraction and g_m is the mesophyll conductance. Leaf transpiration (E) is given by

$$E = 1.6 g_s D, \qquad \text{Eqn 4}$$

where D is the water vapour pressure deficit (VPD) and the factor 1.6 is the ratio of the molecular diffusion coefficients for CO_2 and H_2O. We assume steady-state plant water balance so that E equals the leaf-specific flux of water from the bulk soil to the leaf:

$$E = K_{sl}(\psi_s - \psi_l), \qquad \text{Eqn 5(a)}$$

where ψ_s is the bulk soil water potential and K_{sl} is the total hydraulic conductance between the bulk soil and 1 m^2 of leaf. For resistances in series, K_{sl} satisfies

$$\frac{1}{K_{sl}} = \frac{1}{K_{sr}} + \frac{1}{K_{rl}}, \qquad \text{Eqn 5(b)}$$

where K_{sr} and K_{rl} are the soil-to-root and root-to-leaf hydraulic conductances. K_{sr} is sensitive to soil water potential (e.g. Campbell & Norman, 2000; Duursma *et al.*, 2008); as shown below, this leads to a stomatal closure response to drought (see the Results section). Specifically,

This article is protected by copyright. All rights reserved

Author Manuscript

$$K_{sr} = K_{sr,sat}\left(\frac{\psi_{sat}}{\psi_s}\right)^{2+\frac{3}{b}} \quad \text{Eqn 5(c)}$$

where $K_{sr,sat}$ and ψ_{sat} are the values of K_{sr} and ψ_s for saturated soil, and b depends on soil type. For simplicity, and in order to focus on NSL, we ignore xylem embolism so that K_{rl} is a constant, independent of leaf water potential (but see the Discussion section).

CAP: maximise A assuming leaf water stress-induced reduction in f

According to CAP, A (Eqn 1) is maximised with respect to g_s, where the cost of stomatal opening arises from an assumed reduction in carboxylation capacity (f) induced by a drop in leaf water potential. Also, mesophyll conductance (g_m) is assumed to be infinite so that $c_c = c_i$ (but see the Possible interpretations of CAP and MES subsection below). We assume a reduction factor φ that decreases linearly from 1 to 0 as the leaf water potential ψ_l decreases from 0 to a critical value ψ_c (< 0):

$$\varphi = 1 - \frac{\psi_l}{\psi_c}, \quad \text{Eqn 6}$$

with $\varphi = 0$ if ψ_l is less than ψ_c. In Eqn 1 we then set

$$f = \varphi f_0 \quad \text{Eqn 7(a)}$$

$$c_c = c_i \ , \quad \text{Eqn 7(b)}$$

where f_0 is the value of f in the absence of leaf water stress ($\psi_l = 0$). Eqns 7(a,b) imply that both the initial slope (carboxylation efficiency) and plateau (carboxylation capacity) of the A-c_i curve are a fraction φ of their values in the absence of NSL (Fig. 2a,b). CAP implicitly assumes that the timescales for stomatal responses and for reductions in f are similar.

CAP is a simplified version of the PGENv1.0 model (Friend, 1991), which was itself based on an earlier model of Givnish (1986). In PGENv1.0 the reduction factor φ was assumed to be a sigmoidal function of leaf water potential. By simplifying φ to a linear function of leaf water potential (Eqn 6), the optimal solution for g_s can be obtained analytically without further

This article is protected by copyright. All rights reserved

Author Manuscript

approximation. CAP is also a simplified, analytically-tractable version of the stomatal optimisation model of Hölttä *et al.* (2017), which includes additional features such as xylem embolism, NSL linked to phloem sucrose concentration (as an alternative to leaf water potential, eqn 6) and, consequently, sink limitation to photosynthesis.

MES: maximise *A* assuming leaf water stress-induced reduction in g_m

Like CAP, MES assumes that *A* (Eqn 1) is maximised with respect to g_s, except that the cost of stomatal opening arises from an assumed reduction in g_m rather than *f*. Specifically, MES assumes that

$$f = f_0 \qquad \text{Eqn 8(a)}$$

$$c_c - \Gamma^* = \varphi(c_i - \Gamma^*), \qquad \text{Eqn 8(b)}$$

where φ is the same reduction factor as in CAP (Eqn 6). Eqn 8(b) expresses the assumed reduction in g_m indirectly in terms of its effect on the relationship between c_c and c_i, whereby lower leaf water potential leads to a lower value of c_c relative to c_i; the inclusion of Γ^* in Eqn 8(b) ensures that $c_c = c_i = \Gamma^*$ at the CO_2 compensation point, regardless of the value of the leaf water potential. Our motivation for proposing Eqn 8(b) was two-fold: it is a simple way to encapsulate an effect of leaf water stress on g_m without modelling the underlying mechanistic details, which are largely unknown; and mathematically it reduces to the CAP hypothesis in the limit when c_c tends to Γ^*, when Eqns 1 and 8(a,b) imply that *A* is proportional to $\varphi(c_i - \Gamma^*)f_0$, consistent with Eqns 1 and 7(a,b) in the same limit. In other words, the primary motivation for Eqn 8(b) was model parsimony.

Eqns 8(a,b) imply that the initial slope of the *A*-c_i curve is a fraction φ of its value in the absence of NSL, whereas the plateau value of *A* is unaffected (Fig. 2a,b). However, over the range c_i < 300 μmol mol^{-1} MES and CAP have qualitatively similar effects on the *A*-c_i curve (Fig. 2a). MES implicitly assumes that the timescales for stomatal responses and for reductions in g_m are similar.

Possible interpretations of CAP and MES

CAP and MES (Eqns 7, 8) represent two extremes within a continuum of possible models of NSL to photosynthesis, where NSL occurs entirely through *f* and g_m, respectively. However,

This article is protected by copyright. All rights reserved

Author Manuscript

the interpretation of CAP (Eqns 7a,b) given above, as a reduction in chloroplast carboxylation capacity f combined with infinite g_m, is not the only possibility. By setting $c_c = c_i$ (Eqn 7b), f in Eqn 1 may also be interpreted as an apparent intercellular carboxylation capacity in the presence of a finite g_m, so that Eqn 7(a) may involve reductions in either the actual carboxylation capacity within the chloroplasts or g_m or both. Yet another interpretation of Eqn 7(a) invokes bimodal patchy stomatal closure (Methods S5), in which stomatal-scale carboxylation capacity is equal to its value in the absence of NSL (f_0) and the reduction factor φ represents the fraction of open stomata, so the effective leaf-scale carboxylation capacity is $f = \varphi f_0$.

As noted above, the key assumption of MES (Eqn 8b) was motivated by parsimony rather than by a metabolic understanding of g_m. Nevertheless it is interesting to re-express this assumption directly in terms of g_m itself. When combined with Eqns 1 and 3, Eqn 8(b) is equivalent to

$$g_m = \frac{\varphi}{1-\varphi}\frac{A}{c_c - \Gamma^*} \propto \frac{\varphi}{1-\varphi}[ATP]. \qquad \text{Eqn 9}$$

In the last step we have interpreted $A/(c_c - \Gamma^*)$ as a measure of the concentration of ATP produced by the light reactions of photosynthesis and consumed in the dark reactions (e.g. Thornley & Johnson, 1990, their Eqn 9.12g, where this quantity is denoted X^*). Eqn (9) suggests a metabolic model in which g_m is positively correlated with both leaf water status (via φ) and [*ATP*], rather than with leaf water status alone.

However, in view of current uncertainties about the underlying mechanisms of NSL, we do not adopt any particular mechanistic interpretation of Eqns 7 and 8 beyond their effects on the A-c_i curve (Fig. 2). Rather, we consider CAP and MES as parsimonious hypotheses for NSL to photosynthesis, with the aim of exploring their consequences for stomatal behaviour in the spirit of 'what-if' analysis.

LC: minimise $(a_E E + B)/A$ assuming no non-stomatal limitation to A

According to the Least-Cost hypothesis (LC; Prentice *et al.*, 2014), stomatal conductance minimises the ratio $(a_E E + b_V V_{cmax,0})/A$, where a_E is the sapwood maintenance cost per unit of transpiration, and b_V is the leaf maintenance cost per unit of carboxylation capacity ($V_{cmax,0}$; the subscript 0 denotes the value of V_{cmax} in the absence of NSL), assuming the Farquhar model for

This article is protected by copyright. All rights reserved

Author Manuscript

Rubisco-limited photosynthesis (Farquhar *et al.* 1980, Table 2, Case 7). The total cost $C = a_E E + b_V V_{cmax,0}$ is expressed relative to leaf photosynthesis (A) in the absence of NSL (i.e. $f = f_0$); Prentice *et al.* (2014) also implicitly assumed $c_c = c_i$.

Here we extend the LC hypothesis by considering a generalised cost $a_E E + B$ consisting of a component proportional to E and a component B, independent of E, which depends on the choice of photosynthesis model (Table 2). For the light-limited branch of the Farquhar *et al.* (1980) model (Table 2, Case 11) we assume B is proportional to the light-saturated rate of electron transport ($J_{max,0}$), while for the bi-substrate model (Table 2, Case 3) we assume B is proportional to the carboxylation conductance ($1/r_{x,0}$, i.e. the slope of the linear A-c_c relationship at light saturation, $Q \to \infty$, equivalent to $V_{cmax,0}/k_m$ in the model of Farquhar *et al.*, 1980). In each case B may be interpreted as the cost of maintaining photosynthetic capacity at light saturation.

The assumption by Prentice *et al.* (2014) that the cost term $a_E E$ represents maintenance of sapwood transport structure implies that their version of the LC hypothesis describes stomatal behaviour on timescales of weeks; despite this, it predicts realistic stomatal behaviour on shorter timescales (Prentice *et al.*, 2014; Methods S3). In our extended version of the LC hypothesis, we do not adopt a specific interpretation of the cost term $a_E E$ other than that it represents a cost associated with transpiration. This leaves the possibility of reinterpreting $a_E E$ as some transpiration-related cost on shorter timescales commensurate with CAP and MES. However, exploration of this possibility lies outside the scope of the present study; our aim here is restricted to analysing the intrinsic behaviour of the LC hypothesis based on a generic cost of the form $a_E E + B$.

CF: maximise $A - E/\lambda$ assuming no non-stomatal limitation to A

This is the Cowan–Farquhar (CF) hypothesis (Cowan & Farquhar, 1977) in which A is given by Eqn 1 in the absence of NSL (i.e. $f = f_0$) and we assume infinite mesophyll conductance ($c_c = c_i$; see Volpe *et al.*, 2011 for an application of CF to a model with finite g_m). As already noted, uncertainties surround the determination of λ and the timescale for its variation. Here, for the purposes of comparing CF with CAP and MES, which are hypotheses for short-term stomatal behaviour, we treat λ as an undetermined constant parameter.

Table 2 summarises the four optimisation hypotheses and the three photosynthesis models to which they were applied. We also considered a fifth hypothesis that combines CF and CAP: that is, maximise $A - E/\lambda$ where A incorporates NSL to carboxylation capacity (i.e. f

This article is protected by copyright. All rights reserved

Author Manuscript

= φf_0). The purpose here was to examine the effect of adding NSL to CF or, equivalently, of adding the cost term E/λ to CAP.

Results

The exact analytical solutions for the CAP, MES, CF and LC hypotheses, applied to the generic photosynthesis model of Eqn 1, are derived in Methods S1–S4. Table 3 summarises the key results for stomatal conductance (g_s) and the ratio $(c_i - \Gamma^*)/(c_a - \Gamma^*)$. For MES, results are also given for the ratio of stomatal to mesophyll conductances ($g_s : g_m$) and the CO_2 drawdown $\Delta_C = c_i - c_c = A/g_m$ between the intercellular airspaces and chloroplasts.

Responses of g_s and $c_i : c_a$ to light, VPD and atmospheric CO_2 concentration

Figs 3 and 4 show the predicted responses of g_s and $c_i : c_a$ to light, VPD and CO_2 when the CAP, MES, LC and CF hypotheses are applied to the bi-substrate photosynthesis model (Table 2, Cases 1–4). Overall, the predictions of CAP, MES and LC (Figs 3a–c, 4a–c) are consistent with empirical trends: that is, a saturating stomatal opening response to increasing light (Ng & Jarvis, 1980; Kaufmann, 1982); a strong, nonlinear stomatal closure response to increasing VPD (Morison & Gifford, 1983; Leuning, 1995); a strong, nonlinear stomatal closure response to increasing CO_2 (Morison & Gifford, 1983; Morison, 1987); and a $c_i : c_a$ ratio that decreases with increasing VPD but is relatively insensitive to light and CO_2 (Wong *et al.*, 1979, 1985; Morison & Gifford, 1983; Ball *et al.*, 1987; Leuning, 1995), except at low light and low CO_2 when $c_i : c_a$ tends to 1 as Q tends to zero (Ball & Critchley, 1982; Eamus *et al.*, 1993) or as c_a tends to the CO_2 compensation point Γ^* (Leuning, 1995).

While CF predicts realistic stomatal responses to light and VPD, it predicts an unrealistic peaked response to CO_2, with an opening response at low c_a and a closure response at high c_a (Fig. 3d). CF predicts realistic responses of $c_i : c_a$ to light, VPD and CO_2 (Fig. 4d), except as Q tends to zero. In this limit CF predicts that $c_i : c_a$ tends downwards to a value less than 1; to an extent this behaviour is a result of ignoring leaf mitochondrial respiration, in the presence of which $c_i : c_a$ would tend to 1 at the light compensation point.

We also note that, without its extension to light-dependent photosynthesis models (Table 2, from Case 7 to Cases 3 or 11), LC does not predict the correct limiting response of $c_i : c_a$ at low light. The correct limiting behaviour ($c_i : c_a \to 1$ as $Q \to 0$) requires that the parameter ξ in Eqn 10 below becomes very large at low light; this is true only for Cases 1–3 and 9–11 (Tables 2, 4).

This article is protected by copyright. All rights reserved

Author Manuscript

In contrast to CAP and LC, CF and MES both predict a minimum in $c_i : c_a$ with respect to c_a (Fig. 4d,b), although the latter minimum is less pronounced than the former. Although $c_i : c_a$ is generally observed to be insensitive to c_a, except at low c_a (e.g. Morison & Gifford, 1983), a slightly (+0.03) increase in $c_i : c_a$ was observed in wheat (*Triticum aestivum*) as c_a increased from 225 to 350 μmol mol^{-1} (Polley *et al.*, 1993).

The peaked CO_2 response predicted by CF is a consequence of the cost term E/λ with constant λ, rather than of the choice of photosynthesis model for A

As shown in Methods S4, the peaked g_s-c_a relationship predicted by CF (Fig. 3d) is generic to all photosynthesis models of the form of Eqn 1, irrespective of the values of f and γ. However, the position of the peak in the g_s–c_a curve depends on γ, and in the limiting case of large γ (where A is proportional to $c_c - \Gamma^*$, see Eqn 1) the peaked g_s–c_a response is replaced by an even more unrealistic opening response at all values of c_a, as found previously (Hari *et al.*, 1986; Lloyd & Farquhar, 1994). A peaked g_s–c_a response is also predicted when the CF and CAP hypotheses are combined (Methods S4, data not shown), that is, when NSL is introduced into CF or, equivalently, the cost term E/λ is added to CAP.

In other words, the peaked stomatal CO_2 response predicted by CF is a consequence of the additive cost term E/λ in the CF goal function $A - E/\lambda$ when λ is constant, rather than of the choice of photosynthesis model (A). By contrast, for CAP, MES and LC, the benefit and cost combine multiplicatively, leading to a stomatal closure response to elevated CO_2 at all values of c_a.

Results using the Farquhar *et al*. (1980) photosynthesis model

Qualitatively similar results to Figs 3 and 4 are obtained using the Rubisco- and light-limited branches of the Farquhar *et al.* (1980) photosynthesis model (Table 2, Cases 5–12; data not shown), except that for Rubisco-limited photosynthesis g_s and $c_i : c_a$ are independent of leaf irradiance (Q). In other words, these results are generic to all photosynthesis models of the form given by Eqn 1. However, when applying optimisation to the Farquhar model, additional smoothing assumptions are required to avoid discontinuities between the solutions for the two branches (Friend, 1991; Chen *et al*., 1993; Vico *et al.*, 2013; Buckley *et al.*, 2017).

Further analysis of responses to VPD

A notable feature of the analytical results of Table 3 is that CAP and LC, as well as MES at low

This article is protected by copyright. All rights reserved

Author Manuscript

c_a and CF for large c_a, all predict the same one-parameter relationship between the ratio $(c_i - \Gamma^*)/(c_a - \Gamma^*)$ and VPD (D),

$$\frac{c_i - \Gamma^*}{c_a - \Gamma^*} = \frac{\xi}{\xi + \sqrt{D}}. \qquad \text{Eqn 10}$$

The key difference lies in their predictions for the parameter ξ, which depends on the optimisation hypothesis and the photosynthesis model (Table 4), although CAP and MES (at low c_a) predict the same ξ. From Eqns 4 and 10 it follows that

$$g_s = \left(1 + \frac{\xi}{\sqrt{D}}\right)\frac{A}{c_a - \Gamma^*}. \qquad \text{Eqn 11}$$

In Case 12 (Table 2), for which $\xi = \sqrt{3\lambda\Gamma^*/1.6}$ (Table 4), Eqn 11 reproduces the approximate result for g_s (valid for sufficiently high c_a) derived by Medlyn *et al.* (2011, their Eqn 11 with $c_a - \Gamma^* \approx c_a$, $g_0 = 0$ and $g_1 = \xi$). In Case 7 (Table 2), for which $\xi = b_V(k_m + \Gamma^*)/1.6a_E$ (Table 4), Eqn 10 recovers the exact result for the $c_i : c_a$ ratio derived by Prentice *et al.* (2014, their Eqn 8). The present study shows that Eqns 10 and 11 hold more generally, when CAP, MES (for low c_a), LC (for a general cost function $C = a_E E + B$) and CF (for large c_a) are applied to the generic photosynthesis model in Eqn 1. In the case of CAP and LC, these results hold exactly at all values of c_a, not just for small or large c_a. The reason for the quasi-universality of Eqn 10 is addressed in the Discussion section.

Medlyn *et al.* (2011) found that, for a range of woody species, Eqn 11 explained observed stomatal responses to VPD better than the empirical Ball–Berry model relating g_s to relative humidity (Ball *et al.*, 1987), and as well as the two-parameter Ball–Berry–Leuning model involving the Lohammar function of VPD (Leuning, 1995). Fig. 5 confirms this result using 125 gas exchange datasets assembled by Lin *et al.* (2015).

As already mentioned, Eqns 10 and 11 hold approximately for MES at low c_a. However, as shown in Table 3 and Methods S2, MES also predicts the exact relationship

$$\frac{c_i - \Gamma^*}{c_a - \Gamma^*} = 1 - \frac{E}{E_{\max}}, \qquad \text{Eqn 12}$$

This article is protected by copyright. All rights reserved

Author Manuscript

equivalent to

$$g_s = \left(\frac{E_{\max}}{E}\right)\frac{A}{c_a - \Gamma^*}, \qquad \text{Eqn 13}$$

where $E_{\max} = K_{sl}(\psi_s - \psi_c)$ is the maximum value of E attained when the leaf water potential equals its critical value ($\psi_l = \psi_c$, see Eqn 5a); this occurs in the limit of large VPD. Substituting $E = 1.6Dg_s$ into Eqn 13 and rearranging in terms of g_s yields the alternative form (cf Eqn 11)

$$g_s = \sqrt{\frac{E_{\max}}{1.6D}\frac{A}{c_a - \Gamma^*}}. \qquad \text{Eqn 14}$$

In summary, Eqns 11 and 14, which are exact for CAP and MES, respectively, provide testable predictions by which these two hypotheses might be distinguished.

Relationship between stomatal and hydraulic conductances predicted by CAP and MES, and its implications for drought responses

As shown in Figs 3 and 4, CAP and MES both predict that g_s and $c_i : c_a$ are increasing functions of the soil-to-leaf hydraulic conductance (K_{sl}). The dependence on K_{sl} occurs through the parameter ξ that appears in Eqns 10 and 11 – see Table 4. Algebraic analysis of the results in Table 3 shows that, for both CAP and MES, g_s is to a very good approximation proportional to $K_{sl}^{0.5}$. This result was also obtained numerically from the more complex version of CAP that includes xylem embolism and sink limitation to photosynthesis (Hölttä *et al.*, 2017).

This relationship has implications for the response of g_s to drought, because K_{sl} is sensitive to reductions in soil water content (Eqns 5b,c). This effect is in addition to the direct dependence of g_s on soil water potential through the parameter $a = 1 - \psi_s/\psi_c$ (Table 3) which comes from the NSL reduction factor (Eqn 6). Fig. 6(a) shows that the indirect effect of drought on g_s through a reduction in K_{sl} dominates the direct effect through a reduction in the NSL-related parameter a.

Fig. 6(b) shows that under air or soil drying, leaf water potential never decreases below the critical value ψ_c at which the NSL factor φ is zero (Eqn 6; Fig. 1). This result

This article is protected by copyright. All rights reserved

Author Manuscript

suggests that the extent to which plants exhibit so-called isohydric vs anisohydric drought responses may relate to the NSL reduction factor (φ, Eqn 6), with more anisohydric behaviour corresponding to lower values of ψ_c. This would imply that isohydric and anisohydric behaviours are not discrete possibilities but, rather, belong to a continuum of possible behaviours (parameterised here by ψ_c), as observations suggest (Klein, 2014).

MES predicts coordination of g_s and g_m

As shown in Fig. 3(b,e), MES predicts that g_s and g_m respond similarly under variations in light, VPD and CO_2, broadly consistent with observations (Flexas & Medrano, 2002; Flexas *et al.*, 2008, 2013; Manzoni, 2014; Zhou *et al.*, 2014; Gago *et al.*, 2016; Loucos *et al.*, 2017). The predicted responses of g_m to light and CO_2 in part reflect the underlying assumption of MES (Eqn 8b), which is equivalent to a correlation between g_m, leaf water potential and $A/(c_c - \Gamma^*)$ (Eqn 9), and in part they reflect the outcome of optimising g_s. Further analysis of the results in Table 3 reveals that g_m is, like g_s, approximately proportional to $K_{sl}^{0.5}$. This implies a drought response for both g_s and g_m, as observed (e.g. Galle *et al.*, 2009). The co-ordination of g_m and g_s predicted by MES makes intuitive sense as the emergent outcome of maximising A through an optimal trade-off between increasing g_s and decreasing g_m.

As a result, the stomatal-to-mesophyll conductance ratio (g_s : g_m) is relatively conservative (Fig. 7). Table 3 shows that g_s : g_m is a simple function of the dimensionless parameters $x = (c_i - \Gamma^*)/(c_a - \Gamma^*)$ and $a = 1 - \psi_s / \psi_c$ given by

$$\frac{g_s}{g_m} = \frac{x(1-ax)}{1-x}. \qquad \text{Eqn 15}$$

Eqn 15 implies that $g_s : g_m$ is an increasing function of c_i, consistent with the observed negative response of g_m to increasing c_i being faster than that of g_s (Flexas *et al.*, 2007; Vrábl *et al.* 2009). For well-watered soils ($\psi_s \approx 0$ MPa so that $a \approx 1$), Eqn 15 reduces to the particularly simple result

$$\frac{g_s}{g_m} \approx \frac{c_i - \Gamma^*}{c_a - \Gamma^*}, \qquad \text{(well-watered soil)} \qquad \text{Eqn 16}$$

This article is protected by copyright. All rights reserved

Author Manuscript

so that $g_s : g_m$ is even more conservative under these conditions (Fig. 7b).

MES also makes the following prediction for $\Delta_C = c_i - c_c = A/g_m$, the CO_2 drawdown between the intercellular air spaces and chloroplasts (Table 3):

$$\Delta_C = (c_a - \Gamma^*)x(1 - ax) . \qquad \text{Eqn 17}$$

Eqn 17 describes a peaked function of x with a maximum at $x = 1/2a$. Thus Δ_C may increase, decrease or remain relatively constant in response to environmental or physiological changes. In a meta-analysis of data from 10 studies of 21 herb, shrub and tree species, Δ_C increased in response to drought in 16 out of 23 cases, while Δ_C was approximately constant across four temperate conifer stands with contrasting height (Niinemets *et al.*, 2009). Eqn 17 offers a theoretical basis for explaining these varied responses, through the dependences of x and a on soil-to-leaf hydraulic conductance (K_{sl}) and soil water potential (ψ_s).

In summary, Eqns 15–17 provide novel testable predictions of the MES hypothesis.

Discussion

A quasi-universal relationship between $c_i : c_a$ and VPD

Intriguingly CAP and LC, as well as MES at low c_a and CF at large c_a, all predict the same VPD dependence for $(c_i - \Gamma^*)/(c_a - \Gamma^*)$ (Eqn 10) using quite different goal functions; their predictions differ only in the parameter ξ (Table 4). An explanation for this result is given in Methods S6, which shows that Eqn 10 is a general consequence of optimisation applied to the generic photosynthesis model of Eqn 1, regardless of the specific nature of the optimisation hypothesis. However, only for certain types of optimisation hypotheses is the parameter ξ conservative, leading to conservative behaviour for $(c_i - \Gamma^*)/(c_a - \Gamma^*)$. Methods S6 reveals that, among a large class of conceivable optimisation hypotheses, CAP (in which φ declines linearly with leaf water potential as in Eqn 6) and LC are unique in being the *only* hypotheses, respectively with and without NSL, that predict strictly conservative behaviour for $(c_i - \Gamma^*)/(c_a - \Gamma^*)$. In other words, if stomatal behaviour is indeed the result of optimisation, the observed conservative behaviour of $(c_i - \Gamma^*)/(c_a - \Gamma^*)$ implies that the underlying goal function must be of the CAP or LC type, or close approximations to these (e.g. MES at low c_a, CF at high c_a).

However, because the observed $c_i : c_a$ ratio is not strictly conservative, this

This article is protected by copyright. All rights reserved

Author Manuscript

theoretical result is probably over-restrictive, and there remains considerable uncertainty regarding the precise nature of the costs underlying stomatal opening. In other words, obtaining good fits of Eqn 10 or 11 to observations (Fig. 5) does not, by itself, strongly discriminate between different optimisation hypotheses. Rather, hypotheses differ in their predictions of the parameter ξ in Eqn 10.

Prospects for discriminating between CAP and LC

For the LC hypothesis applied to Rubisco-limited photosynthesis (Table 2, Case 7; Table 4), ξ is proportional to $(b_V / a_E)^{0.5}$. Prentice *et al.* (2014) suggested that b_V (maintenance cost per unit of carboxylation capacity) was fairly conservative, and defined a_E to be the sapwood maintenance respiration cost per unit of transpiration, leading to an expression for a_E in terms of various sapwood characteristics with the result that $\xi_{LC} \propto k_s^{0.5} / h$, where k_s (m^2) is sapwood permeability and h (m) is tree height. The analogous prediction of CAP is $\xi_{CAP} \propto K_{sl}^{0.5}$ (Table 2, Case 5; Table 4).

If we ignore soil hydraulic resistance (well-watered soil) and assume the same relationship of root-to-leaf resistance to sapwood characteristics as Prentice *et al.* (2014), we obtain $\xi_{CAP} \propto (\nu_H k_s/h)^{0.5}$ where ν_H is the Huber value (sapwood:leaf area ratio). The extra factor of $1/h^{0.5}$ in ξ_{LC} compared with ξ_{CAP} reflects the assumption of LC that sapwood maintenance respiration is proportional to h. Also ξ_{LC} does not depend on the Huber value ν_H because this cancels from the ratio of sapwood maintenance respiration to E.

These contrasting predictions might be discriminated using empirical estimates of ξ obtained from fitting Eqn 11 – which is exact for both CAP and LC – to data for trees of different heights and Huber values. However, this comparison may not be valid in drought conditions, when the soil hydraulic conductance becomes an important limiting component of K_{sl}. Moreover, even in well-watered soil, K_{sl} may not scale with h and ν_H as simply as assumed above if, for example, the majority of hydraulic resistance resides elsewhere than in the main stem (Tyree & Ewers, 1991). Therefore, the more direct test of CAP remains the prediction $\xi_{CAP} \propto K_{sl}^{0.5}$. Another avenue for discriminating between CAP (or MES) and LC would be to compare their predicted responses to temperature and altitude (Prentice *et al.*, 2014; Wang *et al.* 2016), taking into account the difference in timescales on which these two hypotheses may operate.

This article is protected by copyright. All rights reserved

Author Manuscript

Prospects for discriminating between CAP and MES

Eqns 10 and 11 on the one hand, and Eqns 12 and 14 on the other hand, are exact predictions of CAP and MES, respectively. These predictions are identical at low c_a, as c_c tends towards Γ^* and A becomes proportional to $\varphi(c_c - \Gamma^*)f_0$ in both hypotheses. However, it may be possible to discriminate between these predictions at high c_a. The basic NSL assumptions of CAP and MES (Eqns 7, 8, Fig. 2) should also be testable directly.

Perspectives for further model development

In the more complex version of CAP solved numerically by Hölttä *et al.* (2017), which includes a xylem vulnerability curve, the model avoided catastrophic xylem cavitation. Also, under drought, soil hydraulic resistance dominated plant resistance. Xylem cavitation therefore had a marginal effect on model behaviour in that study. Indeed, Hölttä *et al.* (2017) found that $g_s \propto K_{sl}^{0.5}$ in agreement with the analytical results for CAP and MES obtained here in the absence of cavitation. Nevertheless it would be of interest to examine the combined effects of NSL and xylem embolism more generally. In particular, the emergent minimum leaf water potential (cf Fig. 6b) might be expected to reflect the more limiting process, NSL or xylem cavitation, that is, whichever has the least negative critical leaf water potential.

Hölttä *et al.* (2017) also considered the hypothesis that the NSL factor φ depends on the phloem sucrose concentration in the source, rather than leaf water potential (Eqn 6), although the two are closely related. This led to additional dependences of g_s on sink strength and phloem hydraulic conductance. It would be of interest to develop an analytically-tractable version of this hypothesis, extended also to MES, in order to gain further insights into its theoretical consequences, in the spirit of the 'what-if' analysis presented here. The effects of including dark respiration, boundary layer conductance and temperature might also be explored.

Conclusion

With reference to the three main aims of the study (see the Introduction section): (1) optimisation hypotheses incorporating NSL to photosynthesis (CAP, MES) predict stomatal and mesophyll conductance responses to above- and below-ground environmental variables that are in broad agreement with observed trends. (2) In a comparison with hypotheses that do not incorporate NSL to photosynthesis (LC, CF), the stomatal responses to aboveground environmental variables predicted by LC are broadly similar to those predicted by CAP and

This article is protected by copyright. All rights reserved

Author Manuscript

MES. CF predicts an unrealistic stomatal response to atmospheric CO_2 concentration, even with NSL to carboxylation capacity included. (3) While it is not yet possible to discriminate between CAP, MES and LC on the basis of current knowledge or data, CAP and MES give rise to novel predictions from which such discrimination may be possible. In particular, MES predicts close coordination of stomatal, mesophyll and hydraulic conductances in forms that are open to further experimental test.

Acknowledgements

Australian Research Council (DP160103436); Academy of Finland (Centre of Excellence 272041, 118780 and Academy Professor 1284701, 1282842); Knut and Alice Wallenberg Foundation (2015.0047); University of Helsinki (AtMath project). We thank Meisha-Marika Holloway-Phillips and Gaby Katul for helpful discussions.

Author contributions

R.D. led the model analysis and wrote the paper. A. Mauranen contributed to the model analysis. A. Mäkelä proposed the MES hypothesis. B.M. extended the LC hypothesis to light-limited photosynthesis and performed the analysis for Fig. 5. T.H. and T.V. proposed the analytical simplification of the model of Hölttä *et al.* (2017) and instigated the research. All authors contributed to developing the research and editing the paper.

References

Ball JT, Woodrow IE, Berry JA. 1987. A model predicting stomatal conductance and its contribution to the control of photosynthesis under different environmental conditions. In: Biggins J, ed. *Progress in photosynthesis research*. Dordrecht, the Netherlands: Martinus-Nijhoff Publishers, 221-224.

Ball MC, Critchley C. 1982. Photosynthetic responses to irradiance by the Grey Mangrove, *Avicennia marina*, grown under different light regimes. *Plant Physiology* **70**: 1101-1106.

Ball MC, Farquhar GD. 1984a. Photosynthetic and stomatal responses of two mangrove species, *Aegiceras corniculatum* and *Avicennia marina*, to long term salinity and humidity conditions. *Plant Physiology* **74**: 1-6.

Ball MC, Farquhar GD. 1984b. Photosynthetic and stomatal responses of the grey mangrove, *Avicennia marina*, to transient salinity conditions. *Plant Physiology* **74**: 7-11.

Buckley TN, Mott KA, Farquhar GD. 2003. A hydromechanical and biochemical model of

This article is protected by copyright. All rights reserved

Author Manuscript

stomatal conductance. *Plant, Cell & Environment* **26**: 1767-1785.

Buckley TN, Sack L, Farquhar GD. 2017. Optimla plant water economy. *Plant, Cell & Environment* **40**: 881-896.

von Caemmerer S, Farquhar GD. 1984. Effects of partial defoliation, changes of irradiance during growth, short term water stress and growth at enhanced p(CO_2) on the photosynthetic capacity of leaves of *Phaseolus vulgaris* L. *Planta* **160**: 320-329.

Campbell GS, Norman JM. 2000. *Introduction to environmental biophysics*. New York, NY, USA: Springer-Verlag.

Chen JL, Reynolds JF, Harley PC, Tenhunen JD. 1993. Coordination theory of leaf nitrogen distribution in a canopy. *Oecologia* **93**: 63-69.

Collatz GJ, Ball JT, Grivet C, Berry JA. 1991. Physiological and environmental regulation of stomatal conductance, photosynthesis and transpiration: a model that includes a laminar boundary layer. *Agricultural and Forest Meteorology* **54**: 107-136.

Cowan IR. 1977. Stomatal behaviour and environment. *Advances in Botanical Research* **4**: 117-228.

Cowan IR. 1982. Regulation of water use in relation to carbon gain in higher plants. In: Lange OL, Nobel PS, Osmond CB, Ziegler H, eds. *Physiological plant ecology. II. Water relations and carbon assimilation.* Berlin, Germany: Springer-Verlag, 589-614.

Cowan IR. 1986. Economics of carbon fixation in higher plants. In: Givnish TJ, ed. *On the economy of plant form and function*. Cambridge, UK: Cambridge University Press, 133-170.

Cowan IR, Farquhar GD. 1977. Stomatal function in relation to leaf metabolism and environment. In: Jennings DH, ed. *Integration of activity in the higher plant*. Cambridge, UK: Cambridge University Press, 471-505.

Dewar RC. 1995. Interpretation of an empirical model for stomatal conductance in terms of guard cell function. *Plant, Cell & Environment* **18**: 365-372.

Dewar RC. 2002. The Ball–Berry–Leuning and Tardieu–Davies stomatal models: synthesis and extension within a spatially aggregated picture of guard cell function. *Plant, Cell & Environment* **25**: 1383-1398.

Dewar RC, Franklin O, Mäkelä A, McMurtrie RE, Valentine HT. 2009. Optimal function explains forest responses to global change. *BioScience* **59**:127-139.

Duursma RA, Kolari P, Perämäki M, Nikinmaa E, Hari P, Delzon S, Loustau D, Ilvesniemi H, Pumpanen J, Mäkelä A. 2008. Predicting the decline in daily maximum

This article is protected by copyright. All rights reserved

Author Manuscript

transpiration rate of two pine stands during drought based on constant minimum leaf water potential and plant hydraulic conductance. *Tree Physiology* **28**: 265-276.

Eamus D, Berryman CA, Duff GA. 1993. Assimilation, stomatal conductance, specific leaf area and chlorophyll responses to elevated CO_2 *Maranthes corymbosa*, a tropical monsoon rain forest species. *Australian Journal of Plant Physiology* **20**: 741-755.

Farquhar GD, von Caemmerer S. 1982. Electron transport limitations on the CO_2 assimilation rates of leaves: a model and some observations in *Phaseolus vulgaris* L. In: Akoyunoglov A, ed. *Proceedings of the 5th International Congress on Photosynthesis*. Philadelphia, PA, USA: Balaban **[Author, please insert page range for proceedings extract]**.

Farquhar GD, von Caemmerer S, Berry JA. 1980. A biochemical model of photosynthetic CO_2 assimilation in leaves of C_3 species. *Planta* **149**: 78-90.

Fisher R, McDowell N, Purves D, Moorcroft P, Sitch S, Cox P, Huntingford C, Meir P, Woodward FI. 2010. Assessing uncertainties in a second-generation dynamic vegetation model caused by ecological scale limitations. *New Phytologist* **187**: 666-681.

Flexas J, Barbour MM, Brendel O, Cabrera HM, Carriquí M, Díaz-Espejo A, Douthe C, Dreyer E, Ferrio JP, Gago J *et al.* 2012. Mesophyll diffusion conductance to CO_2: an unappreciated central player in photosynthesis. *Plant Science* **193**: 70-84.

Flexas J, Diaz-Espejo A, Galmés J, Kaldenhoff R, Medrano H, Ribas-Carbo M. 2007. Rapid variations of mesophyll conductance in response to changes in CO_2 concentration around leaves. *Plant, Cell & Environment* **30**: 1284-1298.

Flexas J, Medrano H. 2002. Drought-inhibition of photosynthesis in C_3 plants: stomatal and non-stomatal limitations revisited. *Annals of Botany* **89**: 183-189.

Flexas J, Ribas-Carbo M, Diaz-Espejo A, Galm ES, Medrano H. 2008. Mesophyll conductance to CO_2: current knowledge and future prospects. *Plant, Cell & Environment* **31**: 602-621.

Flexas J, Scoffoni C, Gago J, Sack L. 2013. Leaf mesophyll conductance and leaf hydraulic conductance: an introduction to their measurement and coordination. *Journal of Experimental Biology* **64**: 3965-3981.

Franklin O, Johansson J, Dewar RC, Dieckmann U, McMurtrie RE, Brännström Å, Dybzinski R. 2012. Modeling carbon allocation in trees: a search for principles. *Tree Physiology* **32**: 648-666.

Friend, AD. 1991. Use of a model of photosynthesis and leaf microenvironment to predict
This article is protected by copyright. All rights reserved

Author Manuscript

optimal stomatal conductance and leaf nitrogen partitioning. *Plant, Cell & Environment* **14**: 895-905.

Friend, AD. 1995. PGEN – an integrated model of leaf photosynthesis, transpiration, and conductance. *Ecological Modelling* **77**: 233-255.

Gago J, de Menezes Daloso D, Figueroa CM, Flexas J, Fernie FR, Nikoloski Z. 2016. Relationships of leaf net photosynthesis, stomatal conductance, and mesophyll conductance to primary metabolism: a multispecies meta-analysis approach. *Plant Physiology* **171**: 265-279.

Galle A, Florez-Sarasa I, Tomas Magdalena, Pou A, Medrano H, Ribas-Carbo, Flexas J. 2009. The role of mesophyll conductance during water stress and recovery in tobacco (*Nicotiana sylvestris*): acclimation or limitation? *Journal of Experimental Botany* **60**: 2379-2390.

Givnish TJ. 1986. Optimal stomatal conductance, allocation of energy between leaves and roots, and the marginal cost of transpiration. In: Givnish TJ, ed. *On the economy of plant form and function*. Cambridge, UK: Cambridge University Press, 171-213.

Guo WD, Guo YP, Liu JR, Mattson N. 2009. Midday depression of photosynthesis is related to carboxylation efficiency decrease and D1 degradation in bayberry (*Myrica rubra*) plants. *Scientia Horticulturae* **123**: 188-196.

Hari P, Mäkelä A, Korpilahti E, Holmberg M. 1986. Optimal control of gas exchange. *Tree Physiology* **2**: 169-175.

Hölttä T, Lintunen A, Chan T, Mäkelä A, Nikinmaa E. 2017. A steady-state model of balanced leaf gas exchange, hydraulics and maximal source–sink flux. *Tree Physiology* **37**: 851-868.

Jarvis PG. 1976. The interpretation of the variations in leaf water potential and stomatal conductance found in canopies in the field. *Philosophical Transactions of the Royal Society of London, Series B. Biological Sciences* **273**: 593-610.

Kaiser E, Morales A, Harbinson J, Kromdijk J, Heuvelink E, Marcelis LF. 2015. Dynamic photosynthesis in different environmental conditions. *Journal of Experimental Botany* **66**: 2415-2426.

Katul G, Manzoni S, Palmroth S, Oren R. 2010. A stomatal optimization theory to describe the effects of atmospheric CO_2 on leaf photosynthesis and transpiration. *Annals of Botany* **105**: 431-442.

Kaufmann, MR. 1982. Leaf conductance as a function of photosynthetic photon flux density
This article is protected by copyright. All rights reserved

Author Manuscript

and absolute humidity difference from leaf to air. *Plant Physiology* **69**: 1018-1022.

Klein, T. 2014. The variability of stomatal sensitivity to leaf water potential across tree species indicates a continuum between isohydric and anisohydric behaviours. *Functional Ecology* **28**: 1313-1320.

Leuning R. 1995. A critical appraisal of a coupled stomatal-photosynthesis model for C_3 plants. *Plant, Cell & Environment* **18**: 339-357.

Lin Y-S, Medlyn BE, Duursma RA, Prentice IC, Wang Ha, Baig S, Eamus D, Resco de Dios V, Mitchell P, Ellesworth D *et al.* 2015. Optimal stomatal behaviour around the world. *Nature Climate Change* **5**: 459-464.

Lloyd J, Farquhar GD. 1994. ^{13}C discrimination during CO_2 assimilation by the terrestrial biosphere. *Oecologia* **99**: 201-215.

Loucos KE, Simonin KA, Barbour MM. 2017. Leaf hydraulic conductance and mesophyll conductance are not closely related within a single species. *Plant, Cell & Environment* **40**: 203-215.

Mäkelä A, Berninger F, Hari P. 1986. Optimal control of gas exchange during drought: theoretical analysis. *Annals of Botany* **77**: 461-467.

Manzoni S. 2014. Integrating plant hydraulics and gas exchange along the drought-response trait spectrum. *Tree Physiology* **34**: 1031-1034.

Manzoni S, Vico G, Palmroth S, Porporato A, Katul G. 2013. Optimization of stomatal conductance for maximum carbon gain under dynamic soil moisture. *Advances in Water Research* **62**: 90-105.

Mediavilla S, Santiago H, Escudero A. 2002. Stomatal and mesophyll limitations to photosynthesis in one evergreen and one deciduous Mediterranean oak species. *Photosynthetica* **40**: 553-559.

Medlyn BE, Duursma R, De Kauwe MG, Prentice IC. 2013. The optimal stomatal response to atmospheric CO_2: alternative solutions, alternative interpretations. *Agricultural and Forest Meteorology* **182-183**: 200-203.

Medlyn BE, Duursma R, Eamus D, Ellsworth DS, Prentice IC, Barton CVM, Crous K, De Angelis P, Freeman M, Wingate L. 2011. Reconciling the optimal and empirical approaches to modelling stomatal conductance. *Global Change Biology* **17**: 2134-2144 (corrigendum **18**: 3476)

Mooney HA, Björkman O, Collatz GJ. 1977. Photosynthetic acclimation to temperature and water stress in the desert shrub *Larrea divaricata*. *Carnegie Institute Washington*

This article is protected by copyright. All rights reserved

Author Manuscript

Yearbook **76**: 328-335.

Morison JIL. 1987. Intercellular CO_2 concentration and stomatal response to CO_2. In: Zeiger E, Cowan IR, Farquhar GD, eds. *Stomatal function*. Stanford, CA, USA: Stanford University Press, 229-251.

Morison JIL, Gifford RM. 1983. Stomatal sensitivity to carbon dioxide and humidity. A comparison of two C_3 and two C_4 grass species. *Plant Physiology* **71**: 789-796.

Nascimento HC, Marenco RA. 2013. Mesophyll conductance variations in response to diurnal environmental factors in *Myrcia paivae* and *Minquartia guianensis* in Central Amazonia. *Photosynthetica* **51**: 457-464.

Ng PAP, Jarvis PG. 1980. Hysteresis in the response of stomatal conductance in *Pinus sylvestris* L. needles to light: observations and a hypothesis. *Plant, Cell & Environment* **3**: 207-216.

Niinemets Ü, Diaz-Espejo A, Flexas J, Galmés J, Warren CR. 2009. Role of mesophyll diffusion conductance in constraining potential photosynthetic productivity in the field. *Journal of Experimental Botany* **60**: 2249-2270.

O'Toole JC, Ozbun JL, Wallace DM. 1977. Photosynthetic response to water stress in *Phaseolus vulgaris. Physiologia Plantarum* **40**: 111-114.

Polley HW, Johnson HB, Marino BD, Mayeux HS. 1993. Increase in C_3 plant water-use efficiency and biomass over Glacial to present CO_2 concentrations. *Nature* **361**: 61-64.

Prentice IC, Dong N, Gleason SM, Maire V, Wright IJ. 2014. Balancing the costs of carbon gain and water transport: testing a new theoretical framework for plant functional ecology. *Ecology Letters* **17**: 82-91.

Sharkey TD. 1984. Transpiration-induced changes in the photosynthetic capacity of leaves. *Planta* **160**: 143-150.

Sitch S, Huntingford C, Gedney N, Levy PE, Lomas M, Piao SL, Betts R, Ciais P, Cox P, Friedlingstein P *et al.* 2008. Evaluation of the terrestrial carbon cycle, future plant geography and climate-carbon cycle feedbacks using five Dynamic Global Vegetation Models (DGVMs). *Global Change Biology* **14**: 2015-2019.

Sperry JS, Alder NN, Eastlack SE. 1993. The effect of reduced hydraulic conductance on stomatal conductance and xylem cavitation. *Journal of Experimental Biology* **44**: 1075-1082.

Sperry JS, Venturas MD, Anderegg WRL, Mencuccini M, Mackay DS, Wang Y, Love DM. 2016. Predicting stomatal responses to the environment from the optimization of

This article is protected by copyright. All rights reserved

Author Manuscript

photosynthetic gain and hydraulic cost. *Plant, Cell & Environment* **40**: 816-830.

Rodriguez-Dominguez CM, Buckley TN, Egea G, Cires A, Hernandez-Santana V, Martorell S, Diaz-Espejo A. 2016. Most stomatal closure in woody species under moderate drought can be explained by stomatal responses to leaf turgor. *Plant, Cell & Environment* **39**: 2014-2026.

Thornley JHM, Johnson IR. 1990. *Plant and crop modelling*. Oxford, UK: Oxford University Press.

Tyree MT, Ewers FW. **1991.** The hydraulic architecture of trees and other woody plants. *New Phytologist* **119**: 345-360.

Vico G, Manzoni S, Palmroth S, Weih M, Katul GG. 2013. A perspective on optimal leaf stomatal conductance under CO_2 and light co-limitations. *Agricultural and Forest Meteorology* **182-183**: 191-199

Volpe V, Manzoni S, Marani M, Katul G. 2011. Leaf conductance and carbon gain under salt-stressed conditions. *Journal of Geophysical Research* **116**: G04035.

Vrábl D, Vašková M, Hronková M, Flexas J, Šantrůček J. 2009. Mesophyll conductance to CO_2 transport estimated by two independent methods: effect of variable CO_2 concentration and abscisic acid. *Journal of Experimental Botany* **60**: 2315-2323.

Wang H, Prentice IC, Davis TW, Keenan TF, Wright IJ, Peng C. 2016. Photosynnthetic responses to altitude: an explanation based on optimality principles. *New Phytologist* **213**: 976-982.

Wolf A, Anderegg WRL, Pacala SW. 2016. Optimal stomatal behaviour with competition for water and risk of hydraulic impairment. *Proceedings of the National Academy of Sciences, USA* **113**: E7222-E7230.

Wong SC, Cowan IR, Farquhar GD. 1979. Stomatal conductance correlates with photosynthetic capacity. *Nature* **282**: 424-426.

Wong SC, Cowan IR, Farquhar GD. 1985. Leaf conductance in relation to rate of CO_2assimilation. 1. Influence of nitrogen nutrition, phosphorus nutrition, photon flux density, and ambient partial pressure of CO_2 during ontogeny. *Plant Physiology* **78**: 821-825.

Wright IJ, Reich PB, Westoby M. 2003. Least-cost input mixtures of water and nitrogen for photosynthesis. *American Naturalist* **161**: 98-111.

Zhang S, Gao R. 2000. Diurnal changes of gas exchange, chlorophyll fluorescence, and stomatal aperture of hybrid poplar clones subjected to midday light stress.
This article is protected by copyright. All rights reserved

Author Manuscript

Photosynthetica **37**: 559-571.

Zhou S, Duursma RA, Medlyn BE, Kelly JWG, Prentice IC. 2013. How should we model plant responses to drought? An analysis of stomatal and non-stomatal responses to water stress. *Agricultural and Forest Meteorology* **182**: 204-214.

Zhou S, Medlyn B, Sabaté S, Sperlich D, Prentice IC. 2014. Short-term water stress impacts on stomatal, mesophyll, and biochemical limitations to photosynthesis differ consistently among tree species from contrasting climates. *Tree Physiology* **34**: 1035-1046.

Supporting Information

Additional Supporting Information may be found online in the Supporting Information tab for this article:

Methods S1 Analytical solution of CAP.

Methods S2 Analytical solution of MES.

Methods S3 Analytical solution of LC.

Methods S4 Analytical solution of CF and CF-CAP.

Methods S5 CAP and stomatal patchiness.

Methods S6 Universality of $(c_i - \Gamma^*)/(c_a - \Gamma^*) = \xi/(\xi + \sqrt{D})$.

Please note: Wiley Blackwell are not responsible for the content or functionality of any supporting information supplied by the authors. Any queries (other than missing material) should be directed to the *New Phytologist* Central Office.

Fig. 1 Schematic depiction of the soil-leaf-atmosphere system, with corresponding CO_2 concentrations (c_a, c_i, c_c), vapour pressure deficit (D), water potentials (ψ_l, ψ_s) and conductances (g_s, g_m, K_{sl}). Model Eqns 1–5 govern the steady-state fluxes of CO_2 (A, red arrows) and H_2O (E, blue arrows). Also shown are Eqns 6–8 describing the assumptions underlying the CAP and MES hypotheses of non-stomatal limitation (NSL, dashed arrows and grey box). f, carboxylation capacity; f_0, value of f in the absence of NSL; ψ_c, critical leaf water potential at which the NSL reduction factor φ is zero; Γ^*, CO_2 photorespiratory compensation point; γ, Michaelis constant for CO_2 fixation. See Table 1 for units and parameter values.

Fig. 2 Hypothesised effects of non-stomatal limitation (NSL) on the curve of leaf

This article is protected by copyright. All rights reserved

Author Manuscript

photosynthesis (A) vs intercellular CO_2 concentration (c_i) for (a) $0 < c_i < 300$ μmol mol^{-1} and (b) $0 < c_i < 2000$ μmol mol^{-1}. Curves are shown for the bi-substrate photosynthesis model (Table 2) with leaf water potential $\psi_l = 0$ MPa (black, no NSL) or $\psi_l = -1$ MPa for MES (orange) and CAP (blue), with all other parameter values given in Table 1. For CAP (Eqns 7a,b), both the initial slope (carboxylation efficiency) and plateau (carboxylation capacity) of the A-c_i curve are a fraction φ (Eqn 6, here 50%) of their values in the absence of NSL. For MES (Eqns 8a,b), the initial slope is reduced as for CAP but the plateau is unchanged.

Fig. 3 Theoretical responses of optimal stomatal (g_s) and mesophyll (g_m) conductances to leaf irradiance (Q, orange), vapour pressure deficit (D, blue) and atmospheric CO_2 concentration (c_a, red). Results for g_s calculated from the exact analytical expressions in Table 3 are shown for the (a) CAP, (b) MES, (c) LC and (d) CF optimisation hypotheses applied to the bi-substrate photosynthesis model (Table 2, Cases 1–4). Also shown for CAP and MES are optimal stomatal responses to changes in soil-to-leaf hydraulic conductance (K_{sl}, dashed black), which also imply stomatal responses to soil drying (see Fig. 6). For both CAP and MES, to a very good approximation g_s is proportional to $K_{sl}^{0.5}$ (except when K_{sl} is very close to zero, where the relationship is linear). (e) Corresponding results for g_m predicted by MES. Each variable was varied independently while all other parameters were kept constant at their default values (Table 1; $Q = 500$ μmol m^{-2} s^{-1}, $D = 10^{-2}$ mol mol^{-1}, $c_a = 400$ μmol mol^{-1}, $K_{sl} = 0.01$ mol m^{-2} s^{-1} MPa^{-1}).

Fig. 4 Theoretical responses of the optimal ratio of intercellular to atmospheric CO_2 concentration ($c_i : c_a$) to leaf irradiance (Q, orange), vapour pressure deficit (D, blue) and atmospheric CO_2 concentration (c_a, red). Results calculated from the exact analytical expressions in Table 3 are shown for the (a) CAP, (b) MES, (c) LC and (d) CF optimisation hypotheses applied to the bi-substrate photosynthesis model (Table 2, Cases 1–4). Also shown for CAP and MES are responses of $c_i : c_a$ to changes in soil-to-leaf hydraulic conductance (K_{sl}, dashed black). Each variable was varied independently while all other parameters were kept constant at their default values (Table 1; $Q = 500$ μmol m^{-2} s^{-1}, $D = 10^{-2}$ mol mol^{-1}, $c_a = 400$ μmol mol^{-1}, $K_{sl} = 0.01$ mol m^{-2} s^{-1} MPa^{-1}).

Fig. 5 Comparison of R^2 values for fits of (a) the empirical Ball–Berry model (BB; Ball *et al.*, 1987), (b) the empirical Ball–Berry–Leuning model (BBL; Leuning, 1995), and the

This article is protected by copyright. All rights reserved

Author Manuscript

optimisation-based relationship of Eqn 11 (with $\Gamma^* = 0$) to 125 gas exchange datasets assembled by Lin *et al.* (2015). For BBL, the parameter D_0 in the VPD-dependent Lohammar function $1/(1 + D/D_0)$ was held constant at 0.03 mol mol^{-1}. Median R^2 values are: BB, 0.594; BBL, 0.648; Eqn 11, 0.646.

Fig. 6 Theoretical responses of optimal stomatal conductance (g_s) and leaf water potential (ψ_l) to soil water potential (ψ_s) and vapour pressure deficit (D). Results are shown for the MES optimisation hypothesis applied to the bi-substrate photosynthesis model (Table 2, Case 2). Similar results are obtained with CAP (Table 2, Case 1, data not shown). (a) Short-dashed curve, direct response of g_s to ψ_s through variation in the parameter $a = 1 - \psi_s/\psi_c$, with soil-to-leaf hydraulic conductance (K_{sl}) held fixed; solid curve, total response of g_s to ψ_s including variations in both a and K_{sl} (Eqns 5b,c). All other parameters were set to their default values (Table 1). (b) Solid curves, corresponding responses of ψ_l to D for ψ_s = –0.1, –0.5 and –1.0 MPa (assuming variable K_{sl}); dashed line, critical leaf water potential (ψ_c) at which the non-stomatal limitation factor (φ, Eqn 6) is zero.

Fig. 7 Theoretical responses of the ratio of stomatal to mesophyll conductances (g_s/g_m) to leaf irradiance (Q, orange), vapour pressure deficit (D, blue), atmospheric CO_2 concentration (c_a, red) and soil-to-leaf hydraulic conductance (K_{sl}, dashed black) predicted by MES applied to the bi-substrate photosynthesis model (Table 2, Case 2). (a) ψ_s = –0.1 MPa: results correspond to the default responses shown in Fig. 3(b) (g_s) and Fig. 3(e) (g_m), with $g_s : g_m$ given by Eqn 15. (b) ψ_s = 0.0 MPa: in this case $g_s/g_m = (c_i - \Gamma^*)/(c_a - \Gamma^*)$ (Eqn 16). Each variable was varied independently while all other parameters were kept constant at their default values (Table 1; Q = 500 μmol m^{-2} s^{-1}, $D = 10^{-2}$ mol mol^{-1}, c_a = 400 μmol mol^{-1}, K_{sl} = 0.01 mol m^{-2} s^{-1} MPa^{-1}).

Table 1 List of symbol definitions, units and default parameter values used in the main text

Symbol	Definition (with Eqn/Table reference)	Units/default value
a	Dimensionless parameter $1 - \psi_s/\psi_c$ (Table 3)	-
a_E	C cost per unit transpiration (LC, Tables 2, 4)	1.0 mol CO_2 mol^{-1} H_2O
A	Leaf photosynthesis (Eqn 1)	mol m^{-2} s^{-1}
b	Soil parameter (Eqn 5c)	4
b_J	C cost per unit $J_{max,0}$ (LC, Tables 2, 4)	mol mol^{-1} e$^-$

This article is protected by copyright. All rights reserved

Author Manuscript

b_V	C cost per unit $V_{cmax,0}$ (LC, Tables 2, 4)	-
b_r	C cost per unit $1/r_{x,0}$ (LC, Tables 2, 4)	-
B	Constant C cost (LC, Table 2)	0.05 mol m^{-2} s^{-1}
c_a	Atmospheric CO_2 concentration (Eqn 2)	400×10^{-6} mol mol^{-1}
c_c	Chloroplast CO_2 concentration (Eqns 1, 3)	mol mol^{-1}
c_i	Leaf intercellular CO_2 concentration (Eqns 2, 3)	mol mol^{-1}
D	Atmospheric water vapour pressure deficit (Eqn 4)	0.01 mol mol^{-1}
E	Leaf transpiration (Eqns 4, 5a)	mol m^{-2} s^{-1}
$E_{\max}$	$K_{sl}(\psi_s - \psi_c)$, maximum value of E (Eqn 5a; Table 3)	mol m^{-2} s^{-1}
f	CO_2-saturated value of A (Eqns 1, 7a)	mol m^{-2} s^{-1}
f_0	Value of f in the absence of NSL (Eqn 7a)	mol m^{-2} s^{-1}
g_s	Stomatal conductance for CO_2 diffusion (Eqn 2, 4)	mol m^{-2} s^{-1}
g_m	Mesophyll conductance (Eqn 3)	mol m^{-2} s^{-1}
$J(Q)$	Electron transport rate (Table 2)	mol e^- m^{-2} s^{-1}
$J_0(Q)$	Value of $J(Q)$ in the absence of NSL (Table 4)	mol e^- m^{-2} s^{-1}
$J_{\max}$	Light-saturated value of $J(Q)$	mol e^- m^{-2} s^{-1}
$J_{\max,0}$	Value of $J_{\max}$ in the absence of NSL (Tables 2, 4)	mol e^- m^{-2} s^{-1}
k_m	Michaelis constant for CO_2 (Tables 2, 4)	mol mol^{-1}
K_{rl}	Root-to-leaf xylem hydraulic conductance (Eqn 5b)	0.01 mol m^{-2} s^{-1} MPa^{-1}
K_{sl}	Soil-to-leaf hydraulic conductance (Eqn 5a,b)	0.01 mol m^{-2} s^{-1} MPa^{-1}
K_{sr}	Soil-to-root hydraulic conductance (Eqn 5b,c)	mol m^{-2} s^{-1} MPa^{-1}
$K_{sr,sat}$	Value of K_{sr} for saturated soil (Eqn 5b)	10^4 mol m^{-2} s^{-1} MPa^{-1}
Q	Leaf photosynthetic photon flux density (Table 2)	500×10^{-6} mol m^{-2} s^{-1}
r_x	Carboxylation resistance (Table 2)	mol^{-1} m^2 s
$r_{x,0}$	Value of r_x in the absence of NSL (Tables 2, 4)	2 mol^{-1} m^2 s
$V_{\max}$	Carboxylation capacity (Table 2)	mol m^{-2} s^{-1}
$V_{\max,0}$	Value of V_{cmax} in the absence of NSL (Tables 2, 4)	mol m^{-2} s^{-1}
w	Parameter in all four analytical solutions (Table 3)	-
x	Ratio $(c_i - \Gamma^*)/(c_a - \Gamma^*)$ (Eqn 10; Table 3)	-
y	Parameter in CF solution (Table 3)	-
z_{CF}	Parameter in CF solution (Table 3)	-
z_{LC}	Parameter in LC solution (Table 3)	-
z_{CAP}	Parameter in CAP and MES solutions (Table 3)	-
α	Photosynthetic quantum yield (Table 2)	mol mol^{-1}

Author Manuscript

This article is protected by copyright. All rights reserved

α_0	Value of α in the absence of NSL (Tables 2, 4)	0.1 mol mol^{-1}
β	Parameter E/E_{max} in MES solution (Table 3)	-
Δ_C	CO_2 drawdown (Eqn 17)	mol mol^{-1}
γ	Michaelis constant for CO_2 (Eqn 1)	mol mol^{-1}
Γ^*	CO_2 photorespiratory compensation point (Eqn 1)	40×10^{-6} mol mol^{-1}
λ	Marginal water loss per C gain (CF, Tables 2, 4)	10^3 mol mol^{-1}
ξ	Parameter in eqn (10) (Table 4)	$mol^{0.5}$ $mol^{-0.5}$
φ	NSL reduction factor (Eqns 6, 7a, 8b)	-
ψ_c	Critical leaf water potential (Eqn 6)	–2 MPa
ψ_l	Leaf water potential (Eqns 5a, 6)	MPa
ψ_s	Soil water potential (Eqns 5a,c)	-2×10^{-3} MPa
ψ_{sat}	Soil water potential at saturation (Eqn 5c)	-2×10^{-3} MPa

C, carbon; NSL, non-stomatal limitation. Parameter values are illustrative only, and do not affect the key conclusions of this study.

Author Manuscript

This article is protected by copyright. All rights reserved

Table 2 Twelve basic combinations of optimisation hypotheses and photosynthesis models considered in this study (Cases 1-12)

	Bi-substrate model[1] $A=\frac{\alpha Q(c_c-\Gamma^*)}{c_c+\alpha Q r_x+\Gamma^*}$ $(f=\alpha Q, \gamma=\alpha Q r_x+\Gamma^*)$	**Farquhar model (Rubisco-limited)**[2] $A=V_{c\max}\frac{c_c-\Gamma^*}{c_c+k_m}$ $(f=V_{c\max}, \gamma=k_m)$	**Farquhar model (light-limited)**[2] $A=\frac{1}{4}J(Q)\frac{c_c-\Gamma^*}{c_c+2\Gamma^*}$ $(f=\frac{1}{4}J(Q), \gamma=2\Gamma^*)$
CAP[3]**: max *A*** $f=\varphi f_0$, $c_c=c_i$	Case 1	Case 5	Case 9
MES: max *A* $f=f_0$, $c_c-\Gamma^*=\varphi(c_i-\Gamma^*)$	Case 2	Case 6	Case 10
LC[4]**: min *C*/*A*** $C=a_E E+B$, $f=f_0$, $c_c=c_i$	Case 3 ($B=b_r/r_{x,0}$)	Case 7 ($B=b_V V_{c\max,0}$)	Case 11 ($B=b_J J_{\max,0}$)
CF[5]**: max *A* – *E*/*λ*** $f=f_0$, $c_c=c_i$	Case 4	Case 8	Case 12

Each photosynthesis model corresponds to the generic model $A=f(c_c-\Gamma^*)/(c_c+\gamma)$ (Eqn 1; c_c, chloroplast CO_2 concentration) with different choices for f and γ as indicated. φ, non-stomatal limitation (NSL) factor (Eqn 6); subscript 0 denotes parameter values in the absence of NSL; c_i, intercellular CO_2 concentration. In CAP, carboxylation capacity (f) is subject to NSL ($f=\varphi f_0$) but γ is not: thus $\alpha=\varphi\alpha_0$ and $r_x=r_{x,0}/\varphi$ so that $\alpha r_x=\alpha_0 r_{x,0}$ is constant (Case 1), $V_{c\max}=\varphi V_{c\max,0}$ (Case 5) and $J_{\max}=\varphi J_{\max,0}$ (Case 9); $c_c=c_i$ (CAP, LC, CF) implies infinite mesophyll conductance. In MES, $c_c-\Gamma^*=\varphi(c_i-\Gamma^*)$ describes the assumed effect of NSL to mesophyll conductance on the relationship between c_c and c_i; LC = Least-Cost hypothesis in which the constant cost (B) depends on the photosynthesis model as indicated (Cases 3, 7 and 11); CF, Cowan–Farquhar hypothesis. See Table 1 for other symbol definitions.

[1]Thornley & Johnson (1990, Eqn 9.12i); [2]Farquhar *et al.* (1980); [3]adapted from Friend (1991) and Hölttä *et al.* (2017); [4]extension of Case 7 (Prentice *et al.*, 2014) to Cases 3 and 11; [5]Cowan & Farquhar (1977).

Author Manuscript

This article is protected by copyright. All rights reserved

Table 3 Exact expressions for $x = (c_i - \Gamma^*)/(c_a - \Gamma^*)$ predicted by the CAP, MES, LC and CF optimisation hypotheses (Table 2), and the corresponding stomatal conductance (g_s)

CAP	$x = \dfrac{1}{1+\sqrt{z_{CAP}}}$	$g_s = \dfrac{f_0}{\gamma+\Gamma^*}\dfrac{xa}{xz_{CAP}+(1-x)(xw+1)}$
MES	$x = 1-\beta$ where $aw\beta^2 = z_{CAP} - \left(\dfrac{\beta}{1-\beta}\right)^2$ $x \approx \begin{cases} \dfrac{1}{1+\sqrt{z_{CAP}}} & (aw \ll 1) \\ 1-\sqrt{\dfrac{z_{CAP}}{aw+1}} & (aw+1 \gg z_{CAP}) \end{cases}$	$g_s = \dfrac{f_0}{\gamma+\Gamma^*}\dfrac{(1-x)a}{z_{CAP}}$ $\dfrac{g_s}{g_m} = \dfrac{x(1-ax)}{1-x}$ $\Delta_C = \dfrac{A}{g_m} = (c_a-\Gamma^*)x(1-ax)$
LC	$x = \dfrac{1}{1+\sqrt{z_{LC}}}$	$g_s = \dfrac{f_0}{\gamma+\Gamma^*}\dfrac{x}{(1-x)(xw+1)}$
CF	$x = \dfrac{1-\sqrt{z_{CF}+y(1-z_{CF})}}{1-z_{CF}}$ $\approx \dfrac{1}{1+\sqrt{z_{CF}}}$ $(y \ll 1)$	$g_s = \dfrac{f_0}{\gamma+\Gamma^*}\dfrac{x}{(1-x)(xw+1)}$

In the case of CAP, LC and CF, the expressions for g_s as functions of x are generally valid independently of optimisation, and depend only on the photosynthesis model and Fick's law; in the case of MES the expression for g_s is only valid at the optimal value of x. These hypotheses are applied to the generic photosynthesis model $A = f(c_c - \Gamma^*)/(c_c + \gamma)$ (Eqn 1), and the predictions for x and g_s are expressed as functions of the dimensionless parameters (see Table 1 for symbol definitions) $a = 1 - \psi_s/\psi_c$, $\beta = E/E_{\max}$, $w = (c_a - \Gamma^*)/(\gamma + \Gamma^*)$, $y = 1.6D/\lambda(c_a - \Gamma^*)$, $z_{CAP} = 1.6Df_0/K_{sl}\,|\psi_c|\,(\gamma + \Gamma^*)$, $z_{CF} = 1.6D/\lambda(\gamma + \Gamma^*)$, and $z_{LC} = 1.6Da_E f_0/B(\gamma + \Gamma^*)$. Approximate expressions for x are also given for the MES and CF hypotheses (valid for small aw and small y, respectively) which have the same general form $x = 1/(1+\sqrt{z})$ as that predicted (exactly) by CAP and LC; this expression is equivalent to $x = \xi/(\xi+\sqrt{D})$ (Eqn 10) where $\xi = \sqrt{D/z}$. MES also predicts the optimal stomatal-to-mesophyll conductance ratio ($g_s : g_m$) and the CO_2 drawdown between the intercellular air spaces and chloroplasts ($\Delta_C = A/g_m = c_i - c_c$) as simple functions of x and a. Table 4 gives expressions for ξ for each of the 12 cases in Table 2. See Supporting Information Methods S1–S4 for details of the mathematical derivations.

Table 4 Expressions for the parameter ξ in the generic prediction

This article is protected by copyright. All rights reserved

Author Manuscript

$(c_i - \Gamma^*)/(c_a - \Gamma^*) = \xi/(\xi + \sqrt{D})$ (Table 3; Eqn 10) for each of the 12 cases in Table 2

	Bi-substrate model	**Farquhar model (Rubisco-limited)**	**Farquhar model (light-limited)**
CAP (exact) and **MES** (for $aw << 1$)	$\sqrt{\frac{K_{sl}\lvert\psi_c\rvert}{1.6}\left(r_{x,0} + \frac{2\Gamma^*}{\alpha_0 Q}\right)}$	$\sqrt{\frac{K_{sl}\lvert\psi_c\rvert}{1.6}\frac{k_m + \Gamma^*}{V_{c\max,0}}}$	$\sqrt{\frac{K_{sl}\lvert\psi_c\rvert}{1.6}\frac{12\Gamma^*}{J_0(Q)}}$
LC (exact)	$\sqrt{\frac{b_r / r_{x,0}}{1.6a_E}\left(r_{x,0} + \frac{2\Gamma^*}{\alpha_0 Q}\right)}$	$\sqrt{\frac{b_V(k_m + \Gamma^*)}{1.6a_E}}$	$\sqrt{\frac{b_J J_{\max,0}}{1.6a_E}\frac{12\Gamma^*}{J_0(Q)}}$
CF (for $y << 1$)	$\sqrt{\frac{\lambda(\alpha_0 Q r_{x,0} + 2\Gamma^*)}{1.6}}$	$\sqrt{\frac{\lambda(k_m + \Gamma^*)}{1.6}}$	$\sqrt{\frac{3\lambda\Gamma^*}{1.6}}$

See Table 1 for symbol definitions; subscript 0 denotes parameter values in the absence of non-stomatal limitation. This prediction (Eqn 10) is exact for CAP and LC, and approximate for MES and CF (valid for small *aw* and small *y*, respectively, where *a*, *w* and *y* are defined in Table 3). For each photosynthesis model, CAP and MES (for $aw << 1$) predict the same ξ.

Author Manuscript

This article is protected by copyright. All rights reserved

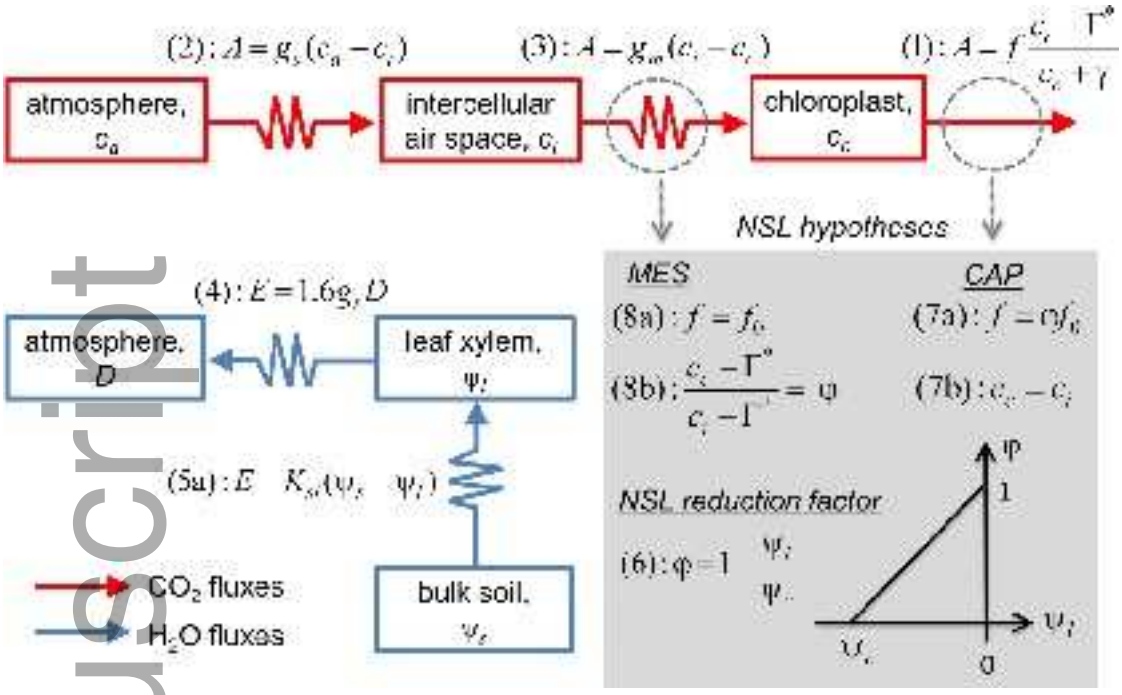

nph_14848_f1.tif

Author Manuscript

This article is protected by copyright. All rights reserved

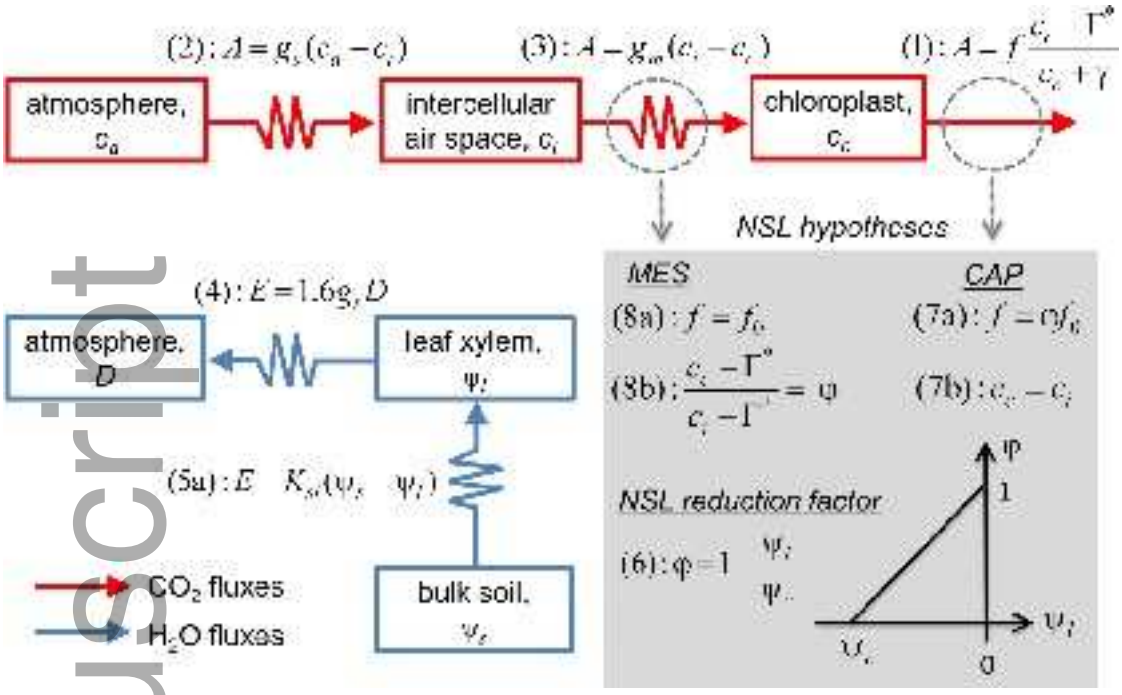

nph_14848_f1.tif

Author Manuscript

This article is protected by copyright. All rights reserved

Author Manuscript

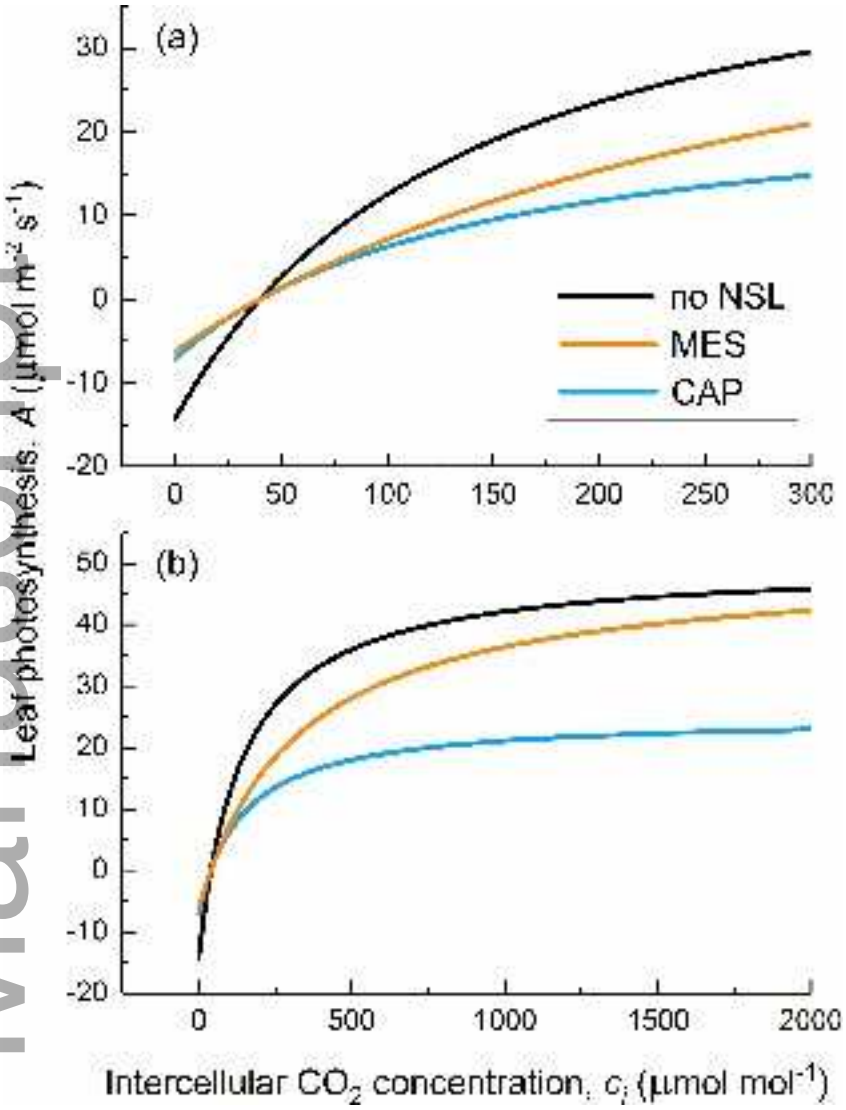

nph_14848_f2.tif

This article is protected by copyright. All rights reserved

Author Manuscript

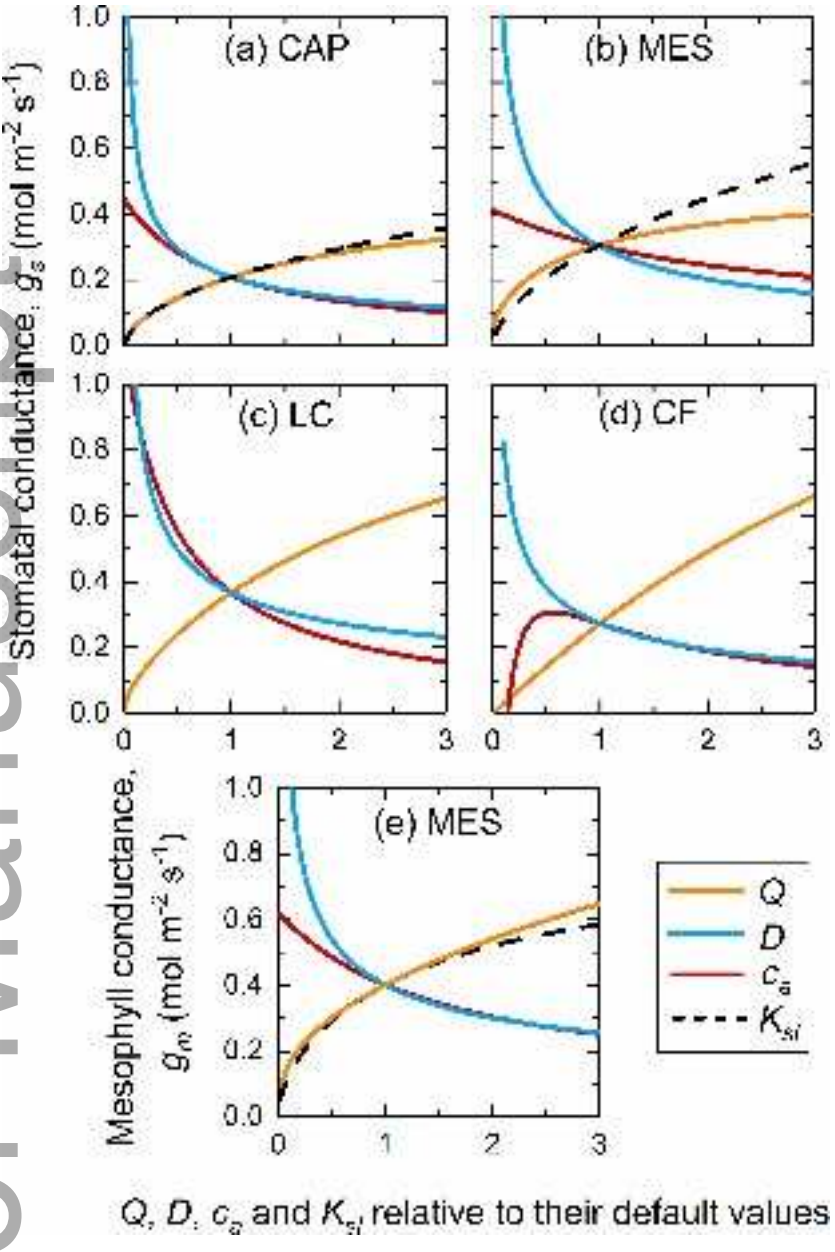

nph_14848_f3.tif

This article is protected by copyright. All rights reserved

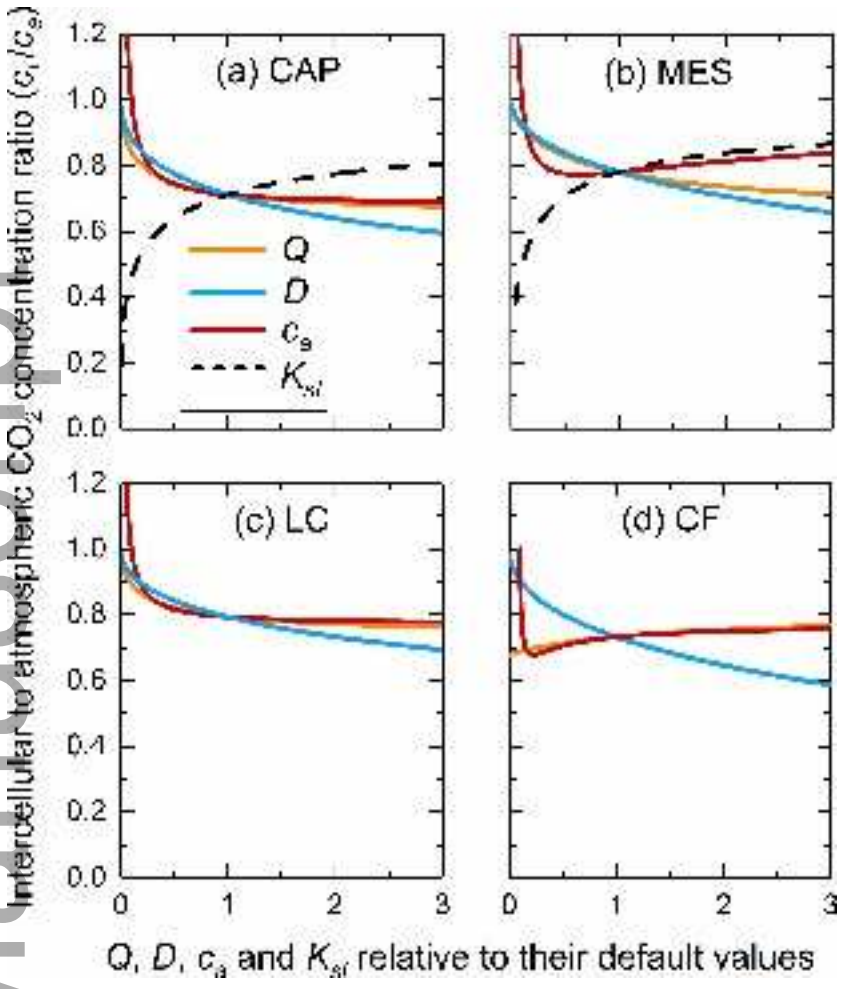

nph_14848_f4.tif

Author Manuscript

This article is protected by copyright. All rights reserved

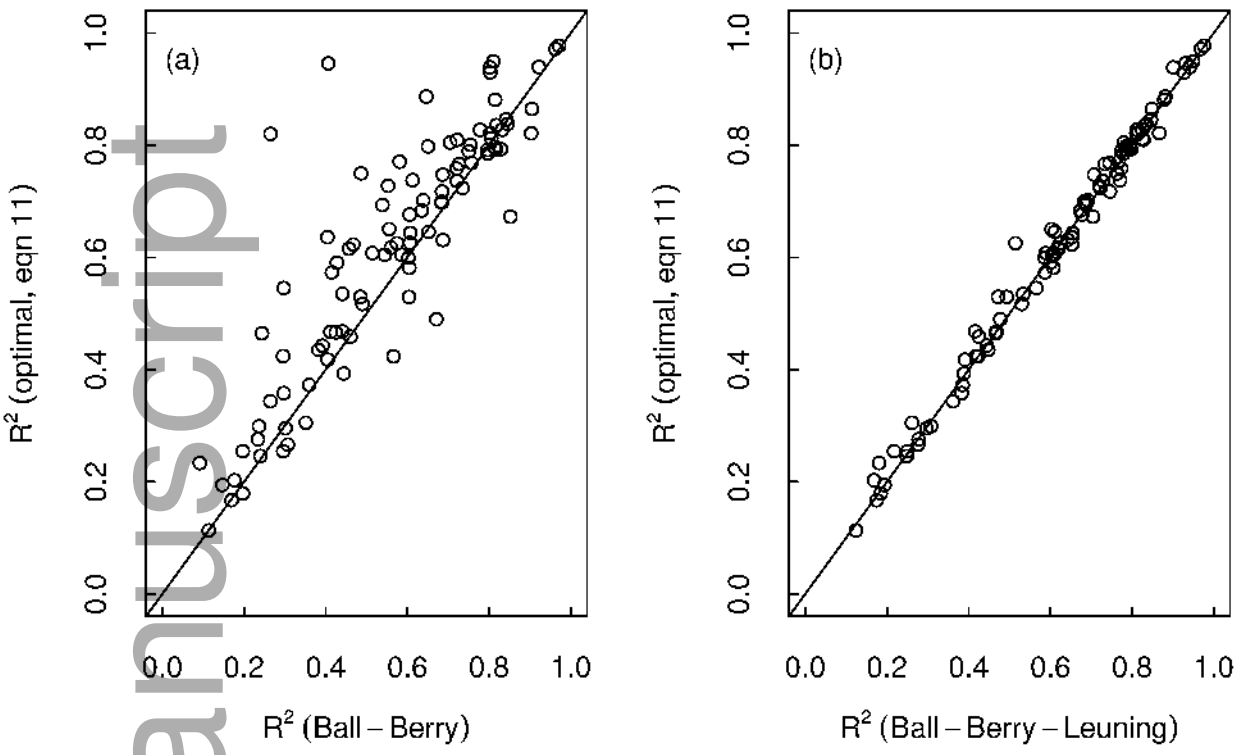

nph_14848_f5.tiff

Author Manuscript

This article is protected by copyright. All rights reserved

Author Manuscript

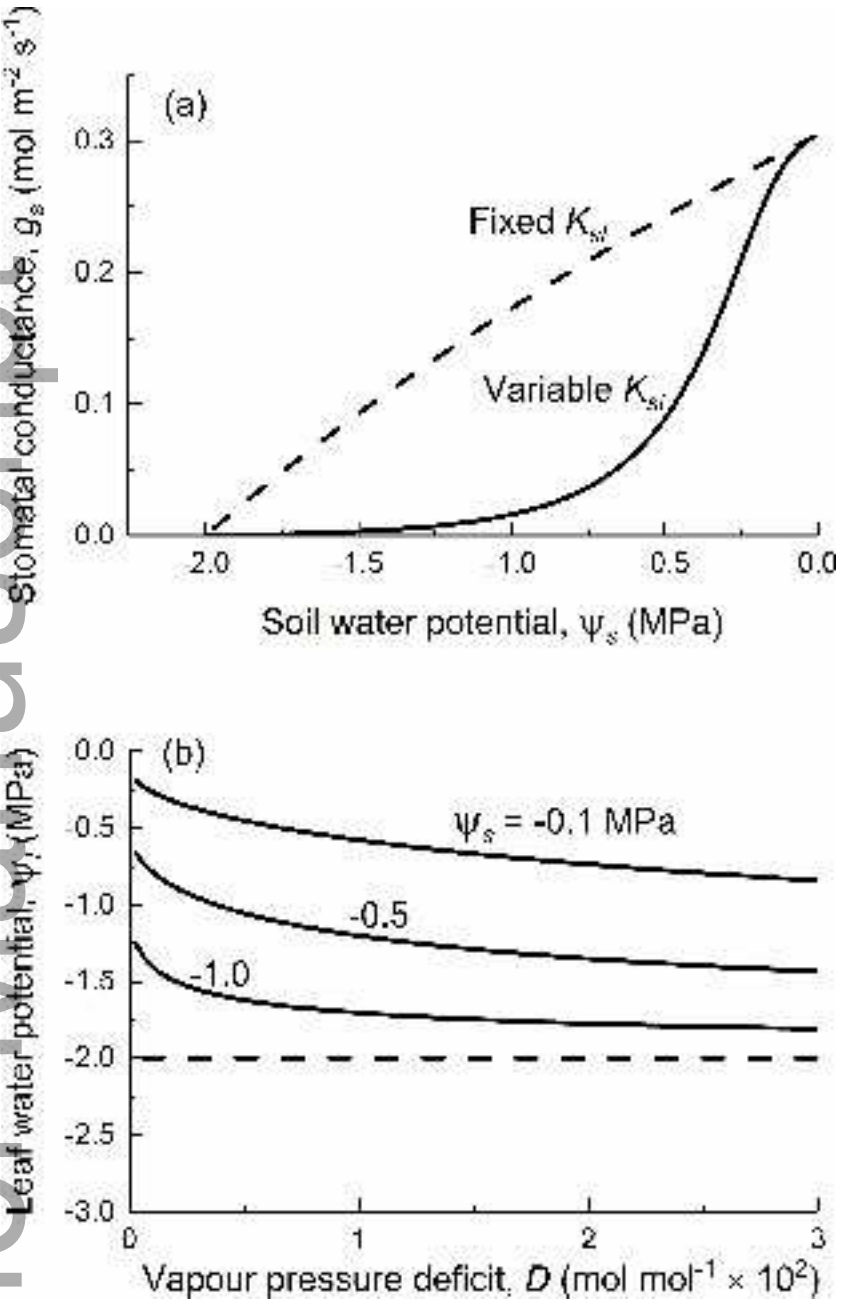

nph_14848_f6.tif

This article is protected by copyright. All rights reserved

Author Manuscript

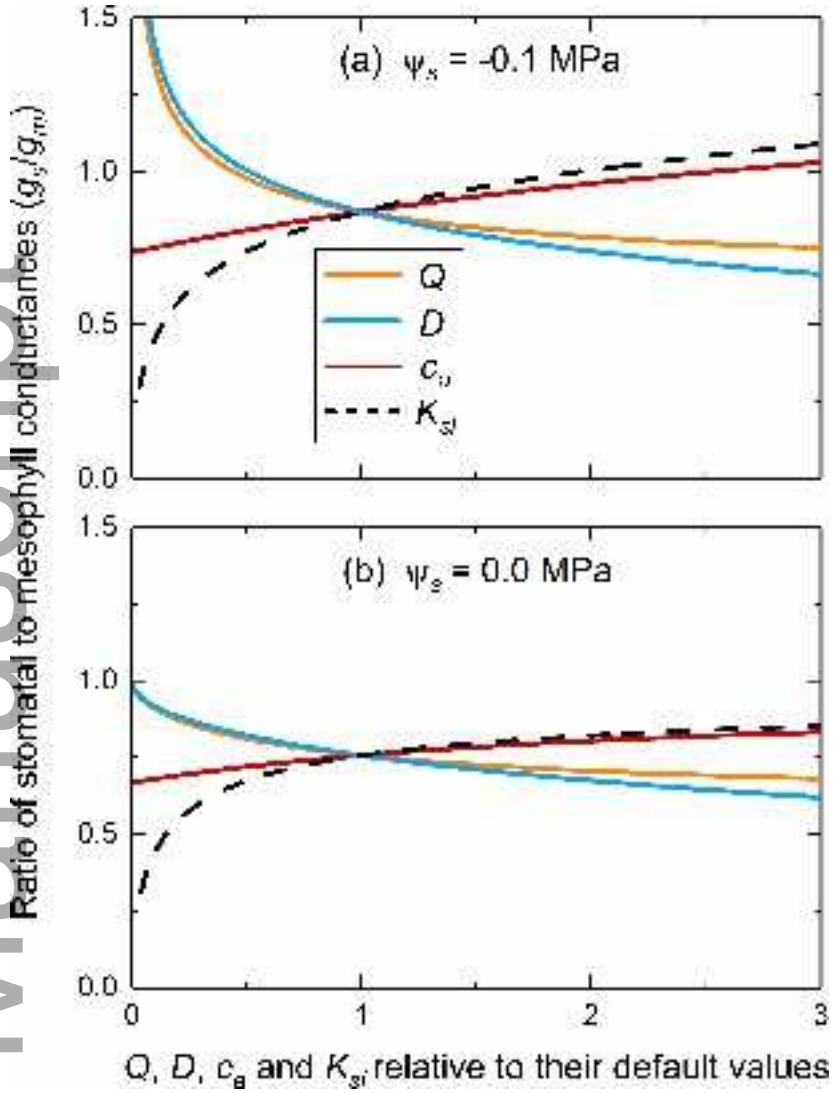

nph_14848_f7.tif

This article is protected by copyright. All rights reserved